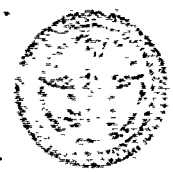

AGARDograph 79

440903

AGARDograph

JET SIMULATION IN GROUND TEST FACILITIES

by

M. PINDZOLA

NOVEMBER 1963

AGARDograph 79

NORTH ATLANTIC TREATY ORGANIZATION

ADVISORY GROUP FOR AERONAUTICAL RESEARCH AND DEVELOPMENT

(ORGANISATION DU TRAITE DE L'ATLANTIQUE NORD)

JET SIMULATION IN GROUND TEST FACILITIES

by

M. Pindzola

November 1983

This is one of a series of publications by the AGARD-NATO Fluid Dynamics Panel.

Professor Wilbur C. Nelson of The University of Michigan is the Editor.

SUMMARY

This paper presents a review of various techniques employed in the simulation of a jet exhaust in ground test facilities. A brief summary of the characteristics of a jet exhausting into both quiescent and moving media is presented. The importance of duplicating the initial inclination angle of the jet, δ_j, when conducting simulation studies is pointed out. Various scaling parameters are enumerated. A requirement for the duplication of the jet pressure ratio, jet momentum, and the parameters $\gamma_j M_j^2/\beta_j$ and $(RT)_j$ is indicated. Experimental data are also presented which verify the importance of these parameters in simulation studies. One method of selecting the geometry and test conditions for a simulation model in order to account for a difference in γ_j between model and full scale and still duplicate the important similarity parameters, is presented.

SOMMAIRE

Ce papier présente une revue de diverses techniques employées dans la simulation de l'échappement du jet, en essais à terre. Un bref sommaire des caractéristiques de l'échappement du jet en milieu calme et agité est présenté. L'importance de doubler l'inclinaison initiale du jet δ_j dans l'étude de la simulation est ponctuée. Différents paramètres d'échelle sont énumérés. Une condition pour la duplication du rapport de pression du jet, de son moment, et des paramètres $\gamma_j M_j^2/\beta_j$ et $(RT)_j$ est indiquée. Des résultats expérimentaux qui vérifient l'importance de ces paramètres en études simulées sont aussi présentés. Aussi est présentée une méthode qui permet de choisir la géométrie et les conditions du test pour une simulation afin de tenir compte d'une différence dans γ_j entre modèle et pleine échelle, tout en cependant doublant les paramètres similaires importants.

533.6.072:533.697.4
3b1c
3b2e2

CONTENTS

	Page
SUMMARY	iii
SOMMAIRE	iii
LIST OF TABLES	vi
LIST OF FIGURES	vi
NOTATION	viii
I. INTRODUCTION	1
II. JET FLOW CHARACTERISTICS	1
1. JETS EXHAUSTING INTO A MEDIUM AT REST	2
1.1 Initial Inclination of the Jet Boundary	3
1.2 Jet Boundary Shapes	5
1.3 Intercepting Shock Boundary	6
1.4 Primary Wavelength of the Jet	7
1.5 Distance to the First Mach Disc	7
1.6 Jet Mixing Region	7
1.7 Jet Noise	8
2. JETS EXHAUSTING INTO A MOVING STREAM	9
2.1 Initial Inclination of the Jet Boundary	10
2.2 Jet Boundary Shapes	11
2.3 Jet Mixing Region	12
2.4 Jet Shock Reflection	12
III. SCALING PARAMETERS	13
3. JET BOUNDARY SIMULATION	13
4. JET SHOCK SIMULATION	14
5. SIMULATION OF JET FLOW PARAMETERS	15
5.1 Jet Mass Flow	15
5.2 Jet Kinetic Energy	15
5.3 Jet Internal Energy	16
5.4 Jet Enthalpy	16
5.5 Jet Momentum	16
5.6 Jet Thrust	17
6. BASE HEATING SIMULATION PARAMETERS	17
7. JET MIXING SIMULATION	17
8. JET NOISE SIMULATION	18

	Page
IV. METHODS OF JET SIMULATION	19
9. COLD GAS JETS	19
9.1 Air	19
9.2 Helium	19
9.3 Carbon Dioxide	19
10. COLD GAS MIXTURES	19
11. HOT GAS JETS	20
11.1 Hot Air	20
11.2 Hydrogen and Air	20
11.3 Hydrogen Peroxide	20
11.4 Turbojet Simulator	20
12. ROCKET MOTOR SIMULATORS	21
V. EXPERIMENTAL RESULTS	21
13. JET EXIT EFFECTS	21
13.1 Initial Inclination of the Jet Boundary	22
13.2 Base Pressure	22
13.3 Exit Shock Position	22
14. DOWNSTREAM EFFECTS	23
14.1 Transmitted Shock Position	23
14.2 Transmitted Shock Strength	23
14.3 Transmitted Shock Angle	23
14.4 Jet Boundary Shape	24
14.5 Jet Momentum Effects	24
VI. DISCUSSION	24
15. JET EXIT EFFECTS	24
16. DOWNSTREAM EFFECTS	25
17. ADDITIONAL REMARKS	25
VII. REFERENCES AND BIBLIOGRAPHY	26
TABLES	32
FIGURES	36
DISTRIBUTION	

LIST OF TABLES

		Page
TABLE I	Summary of Scaling Parameters	32
TABLE II	Properties of Gaseous Media	33

LIST OF FIGURES

Fig.1	Effect of jet Mach number on the initial inclination angle of a jet exhausting into a medium at rest	
	(a) $\gamma_j = 1.667$	34
	(b) $\gamma_j = 1.38$	35
	(c) $\gamma_j = 1.25$	36
	(d) $\gamma_j = 1.133$	37
Fig.2	Effect of the ratio of specific heats of the jet on the initial inclination angle of a jet exhausting into a medium at rest	38
Fig.3	Effect of the ratio of specific heats of the jet on the initial inclination angle of a jet exhausting into a vacuum	39
Fig.4	Comparison of initial inclination angle of a jet exhausting into a medium at rest calculated by an exact and an approximate series solution	40
Fig.5	Effect of the ratio of specific heats of the jet on the boundary of a jet exhausting into a medium at rest	41
Fig.6	Effect of the jet pressure ratio on the boundary of a jet exhausting into a medium at rest	42
Fig.7	Effect of jet Mach number on the boundary of a jet exhausting into a medium at rest	43
Fig.8	Effect of jet Mach number on the spreading rate parameter of a jet exhausting into a medium at rest	44
Fig.9	Effects on jet noise of a subsonic jet exhausting into a medium at rest	45
Fig.10	Effect of jet Mach number on the initial inclination angle of a jet exhausting into a moving stream	46
Fig.11	Effect of the ratio of specific heats of the jet on the initial angle of a jet exhausting into a moving stream	47
Fig.12	Effect of free stream Mach number of the initial inclination angle of a jet exhausting into a moving stream	48

Page

Fig.13 Effect of free stream Mach number on the boundary of a jet exhausting into a moving stream 49

Fig.14 Typical Schlieren photograph of a jet exhausting into a moving stream 50

Fig.15 Comparison of an experimental and calculated jet shock in a jet exhausting into a moving stream 51

Fig.16 Values of the initial inclination angle of a jet exhausting into a medium at rest using a constant jet Mach number similarity parameter

(a) $(p_j/p_\infty - 1)\dfrac{1}{\gamma_j} = 2.4$ 52

(b) $(p_j/p_\infty - 1)\dfrac{1}{\gamma_j} = 31.2$ 53

Fig.17 Values of the initial inclination angle of a jet exhausting into a medium at rest using a constant jet pressure ratio similarity parameter, $\gamma_j M_j^2/\beta_j = 3.98$ 54

Fig.18 Initial inclination angle of a sonic jet exhausting into a moving stream 55

Fig.19 Effect of a sonic jet exhaust on base pressure 55

Fig.20 Effect of the exit shock from a sonic jet on the pressure coefficient at a point in a moving stream 56

Fig.21 Effect of the transmitted shock from a sonic jet on the pressure coefficient at a point in a moving stream 56

NOTATION

Symbol		*Dimensions*
a	speed of sound	L/t
A	area	L^2
c	specific heat	L^2/t^2T
C	coefficient	None
d	diameter	L
F	thrust or force	F
k	shock reflection parameter	None
L	length	L
m	mass	m
M	Mach number	None
p	static pressure	F/L^2
q	dynamic pressure	F/L^2
R	gas constant or radius	L^2/t^2T or L
t	time	t
T	temperature	T
u	velocity in the x direction	L/t
V	velocity	L/t
w	sound power	mL^2/t^3
x, r	coordinates in the axial and radial directions	L
β	$(M^2 - 1)^{\frac{1}{2}}$	None
λ	Kawamura parameter	None
γ	ratio of specific heats	None
δ	flow inclination angle	None

Symbol		*Dimensions*
θ	geometric angle	None
μ	Mach angle	None
ν	turning angle from $M = 1$ to $M > 1$	None
ρ	density	m/L^3
σ	experimental constant	None

Subscripts

b	jet boundary
B	boat-tail or base
f	full scale
F	thrust
j	conditions at the jet nozzle exit
m	model
md	Mach disc
N	nozzle
p	at constant pressure
s	intercepting shock boundary
t	total or stagnation
v	at constant volume
∞	free stream
1	conditions before expansion or compression
2	conditions after expansion or compression
*	conditions at the nozzle throat

JET SIMULATION IN GROUND TEST FACILITIES

M. Pindzola*

I. INTRODUCTION

Shortly after the inception of the use of jet propulsion for air vehicles, it was observed that significant changes were realized between the jet-on and jet-off cases on the aerodynamic and thermodynamic characteristics of the vehicle. Early summaries of these effects are presented in References 1 and 2 for aircraft and missile configurations respectively. Since these summaries were published, many additional investigations have been conducted in order to more accurately define the jet interactions. Some of the more recent studies are listed as References 3 to 10 in this Report. Each of these references in turn lists the most recent work in the respective fields of study.

The purpose of this Report is to summarize the various techniques which are used to obtain the jet-on characteristics. Results of such investigations will be quoted only to show the merit of the techniques employed.

The discussion will be limited primarily to an axisymmetric, under-expanded jet. A short review of the characteristics of such a jet are presented in Section II. This review is separated into the categories of a jet exhausting into a medium at rest and into a moving stream. It should be realized that even with a vehicle in motion, portions of the jet exhaust for certain base configurations can be typified as though exhausting into a medium at rest.

In Section III, some of the scaling laws of particular concern to the subject matter are presented. No discussion of the more usual fluid dynamic and thermodynamic similarity parameters such as the Reynolds and Prandtl numbers is presented.

Methods of jet simulation used in ground test facilities are next presented in Section IV followed by a presentation of typical test results using these techniques in Section V. The more important aspects of these results are discussed in Section VI.

The bibliography at the conclusion of the Report is categorized according to the subject matter of the various sections of the Report.

II. JET FLOW CHARACTERISTICS

The study of the characteristics of the flow of a jet of gas into a surrounding medium has received much attention since the work of St. Venant and Wantzel in 1839. A comprehensive summary of these studies up to 1954 is given by Pai in Reference 11. In order to keep the references in this Report within bounds, those listed in Pai's publication will not be repeated here.

---

*ARO, Inc., USAF Arnold Engineering Development Center, Tullahoma, Tennessee, U.S.A.

The initial structure of an axisymmetric jet consists of a core surrounded by an annular mixing region. Farther downstream, the entire jet is a mixing region. Theories to predict this jet structure have been developed under the assumption of either inviscid or viscous considerations.

For jets in which the ratio of the pressure at the exit of the jet nozzle to the ambient pressure of the surrounding medium is low, inviscid theories based on the linearized equations of fluid flow (Refs.12 to 19) are used to describe the jet characteristics. Since these derivations are not applicable at high exit to ambient pressure ratios, resort is made to the method of characteristics (Refs.20 to 23) or to approximate solutions based on various assumptions (Refs.24 to 29).

Although the inviscid theories have been fairly successful in predicting the jet structure immediately downstream of the jet exit, resort must be made to viscous theories (Refs.30 to 37) to obtain jet characteristics further downstream. In these cases, the fluid flow equations based on the boundary layer approximations are used assuming either laminar or turbulent mixing.

Various experimental studies (Refs.38 to 45) have also been made to determine the structure of jets and to serve as a check on the validity of the theoretical analyses. From both the analytical and experimental studies of gas jets, the following information is derived.

1. JETS EXHAUSTING INTO A MEDIUM AT REST

A sketch of the generalized flow pattern of an under-expanded (over-pressured) axisymmetric jet exhausting into a medium at rest is shown below:

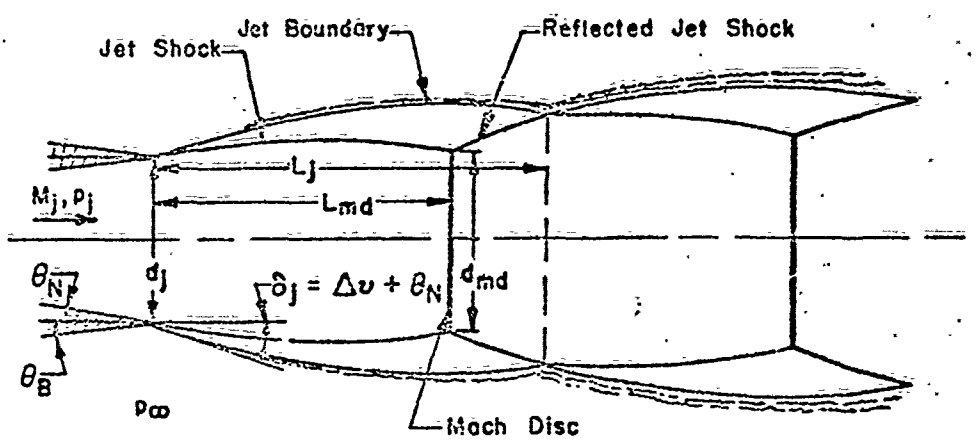

As the jet emerges from the nozzle, it expands to the pressure of the surrounding medium at the jet boundary. The condition of constant pressure at the boundary causes the curvature of the boundary to tend back toward the axis of the flow. The jet shock is formed by the coalescense of the compression waves required to turn the flow at the boundary. For a slightly under-expanded jet, the jet shocks meet to form a shock

diamond. However, as the nozzle pressure ratio is increased, a Mach reflection occurs in the jet forming a Mach or shock disc. A reflection of the jet shock occurs in either case, and the pattern is repeated at the intersection of the reflected shock and the jet boundary.

The study of the jet structure thus involves the prediction of the above pattern as influenced by the various variables such as the nozzle pressure ratio, jet Mach number, ratio of specific heats of the jet, and so forth. Near the exit of the nozzle, the effects of viscosity are small and inviscid theories describe the flow reasonably well. However, further downstream from the exit the mixing region between the jet and free stream predominates and viscous theories are required.

1.1 Initial Inclination of the Jet Boundary

In exhausting from the pressure at the exit of the nozzle, p_j, to a lower ambient pressure, p_∞, the jet will initially undergo a two-dimensional expansion at the nozzle lip. This expansion is governed by the Prandtl-Meyer equations. In expanding from a Mach number of 1.0 to a higher Mach number, M, the relationship between the turning angle ν and M is given by

$$\nu \equiv \sqrt{\frac{\gamma+1}{\gamma-1}} \arctan\sqrt{\frac{\gamma-1}{\gamma+1}\beta} - \arctan\beta , \qquad \text{(II-1)}$$

The angle required for expansion from some initial supersonic Mach number, M_1, to some higher Mach number, M_2, is simply the difference in the values of ν at the two Mach numbers, i.e.

$$\Delta\nu \equiv \nu_2 - \nu_1 . \qquad \text{(II-2)}$$

The ratio of the final to initial static pressures is given by

$$\frac{p_2}{p_1} = \left[\frac{2 + (\gamma-1)M_1^2}{2 + (\gamma-1)M_2^2}\right]^{\frac{\gamma}{\gamma-1}} . \qquad \text{(II-3)}$$

For a jet exhausting into a medium at rest, the jet exit conditions (denoted by the subscript j) become the conditions before the expansion (subscript 1) and the free-stream pressure p_∞ is the pressure after the expansion, p_2. For values of γ_j equal to 1.667, 1.38, 1.25 and 1.133, an explicit relationship for $\Delta\nu$ in terms of β_j and p_j/p_∞ can be determined. For these values of γ_j, Equations (II-1) and (II-3) reduce to the following:

For $\gamma_j = 5/3 = 1.667$.

$$\tan\nu = \frac{\beta^3}{4 + 3\beta^2} \qquad \text{(II-4)}$$

$$\beta_2^2 = \left(\frac{p_1}{p_2}\right)^{0.4}(\beta_1^2 + 4) - 4 . \qquad \text{(II-5)}$$

In terms of β_j and p_j/p_∞, Equations (II-4) and (II-5) can be combined to give

$$\tan\Delta\nu = \frac{\left[\left(\frac{p_j}{p_\infty}\right)^{0.4}(\beta_j^2+4)-4\right]^{3/2}(3\beta_j^2+4) - 3\left(\frac{p_j}{p_\infty}\right)^{0.4}(\beta_j^2+4)\beta_j^3 + 8\beta_j^3}{\left[\left(\frac{p_j}{p_\infty}\right)^{0.4}(\beta_j^2+4)-4\right]^{3/2}\beta_j^3 + 3\left(\frac{p_j}{p_\infty}\right)^{0.4}(\beta_j^2+4)(3\beta_j^2+4) - 8(3\beta_j^2+4)} \qquad \text{(II-6)}$$

For $\gamma_j = 29/21 = 1.38$

$$\tan\nu = \frac{(\beta^3 - 1.25\beta)(6.25+\beta^2)^{\frac{1}{2}} + 3.125\beta + 6.5\beta^3}{(6.25+4\beta^2)(6.25+\beta^2)^{\frac{1}{2}} + 11.25\beta^2 + 15.625 - \beta^4} \qquad \text{(II-7)}$$

$$\beta_2^2 = \left(\frac{p_1}{p_2}\right)^{0.276}(\beta_1^2+6.25) - 6.25 . \qquad \text{(II-8)}$$

For $\gamma_j = 5/4 = 1.25$

$$\tan\nu = \frac{8\beta^3}{27+18\beta^2-\beta^4} \qquad \text{(II-9)}$$

$$\beta_2^2 = \left(\frac{p_1}{p_2}\right)^{0.2}(\beta_1^2+9) - 9 . \qquad \text{(II-10)}$$

For $\gamma_j = 17/15 = 1.133$

$$\tan\nu = \frac{\beta^3(80-\beta^2)}{256+160\beta^2-15\beta^4} \qquad \text{(II-11)}$$

$$\beta_2^2 = \left(\frac{p_1}{p_2}\right)^{0.1177}(\beta_1^2+16) - 16 . \qquad \text{(II-12)}$$

Curves showing the effects of jet Mach number, M_j, and pressure ratio, p_j/p_∞, on the turning angle of the jet flow, $\Delta\nu$, for the above values of γ_j are presented in Figures 1 and 2.

The limiting values of $\Delta\nu$ which represent the turning angles when exhausting into a vacuum are shown in Figure 3. These values of $\Delta\nu$ are approached when considering problems associated with the exploration of space (see Ref.45 for example).

In addition to the parameters mentioned above (i.e., p_j/p_∞, γ_j and M_j), the initial inclination angle of the jet, δ_j, also depends on the nozzle exit angle and is given by:

$$\delta_j = \theta_N + \Delta\nu \qquad \text{(II-13)}$$

Thus a fourth parameter is available and often used to obtain matched conditions of the initial inclination angle of a jet.

For small values of the angle, $\Delta\nu$, the ratio of the free stream static pressure and the jet exit static pressure can be expressed by the following series:

$$\frac{p_\infty}{p_j} = 1 - \frac{\gamma_j M_j^2}{\beta_j}(\Delta\nu) + \gamma_j M_j^2 \frac{(\gamma_j+1)M_j^2 - 4\beta_j^2}{4\beta_j^4}(\Delta\nu)^2$$

$$- \frac{\gamma_j M_j^2}{2\beta_j^7}\left[\frac{\gamma_j+1}{6}M_j^8 - \frac{5+7\gamma_j-2\gamma_j^2}{6}M_j^6\right.$$

$$\left. + \frac{5}{3}(\gamma_j+1)M_j^4 - 2M_j^2 + \frac{4}{3}\right](\Delta\nu)^3 + \ldots\ldots \qquad \text{(II-14)}$$

The pressure ratio range for which Equation (II-14) is applicable can be deduced from the curves of Figure 4. The curves labeled 1st, 2nd and 3rd are obtained by retaining the corresponding terms of the equation.

1.2 Jet Boundary Shapes

The shape of the jet boundary for the first few diameters downstream of the nozzle exit can be assumed to be affected only slightly by viscous effects and therefore can be determined by inviscid solutions. The method of characteristics is thus generally used as an 'exact' solution for the jet boundary and various approximate techniques are employed to duplicate the characteristic solution.

Approximately 3000 boundaries determined by the method of characteristics over the range of the parameters used in the previous discussion of initial angles are presented in Reference 20. A few of these are reproduced in Figures 5, 6 and 7 in order to show the effects of the parameters.

It was shown in Reference 20 that a circular arc of constant radius, R_b, provides an adequate approximation to the jet boundary up to the point of maximum diameter provided this point can be determined in advance. However, no suitable method for accurately predicting the maximum jet diameter and its location has as yet been determined.

The results of a spreading study of an air jet at high altitudes reported in Reference 27 indicate that an approximate location of the jet boundary can be obtained by the following technique. With reference to the sketch overleaf, after determining the initial inclination angle of the jet from Equation (II-13), a line is constructed perpendicular to this tangent to the jet boundary. The boundary radius, R_b, for $\gamma_j = 1.4$ is determined from the following equation:

$$\frac{R_b}{r_j} = 38.4\frac{\epsilon_s}{M_j} = \frac{15.7}{M_j}\sqrt{5+M_j^2}\,. \qquad \text{(II-15)}$$

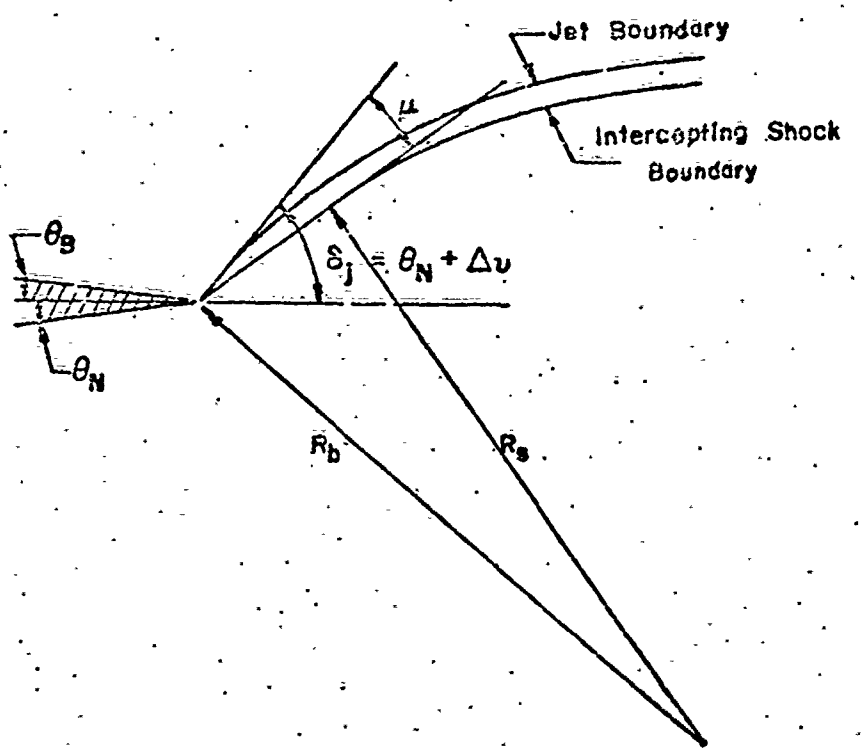

This radius is located along the perpendicular and the jet boundary is drawn as a circular arc. Assuming that the radius ratio is proportional to a_∞/u_j for γ_j other than 1.4, R_b for other γ_j can be obtained by using the $\gamma_j = 1.4$ radius ratio as a reference value at a particular M_j and substituting into the following equation (see Eqn. (19) in Ref. 27):

$$\frac{R_b}{r_j} = \left(\frac{R_b}{r_j}\right)_{1.4} \sqrt{\frac{(\gamma_j + 1)(5 + M_j^2)}{12 + 6(\gamma_j - 1)M_j^2}} \quad \text{(II-16)}$$

Other approximate techniques for calculating the jet boundary exhausting into a medium at rest are summarized in Reference 28.

1.3 Intercepting Shock Boundary

The jet boundary calculations in Reference 20 by the method of characteristics also defined the jet or intercepting shock boundary within the jet boundary. This boundary (see previous sketch) is initially tangential to the final Mach line of the expansion fan and is then formed by the reflection of the expansion fan waves from the jet boundary.

In Reference 28 a circular arc approximation for the intercepting shock (see sketch) is given with the radius of curvature given by

$$R_s = R_b \cos\mu \quad \text{(II-17)}$$

where $$\mu = \arcsin \frac{1}{M_2} .$$

Thus, again if a method of determining R_b is available, an approximation to the jet shock boundary can be obtained readily.

1.4 Primary Wavelength of the Jet

Many investigators have attempted to derive an analytical expression for the primary wavelength of a jet, L_j, that is, the length of the first periodic jet structure. For values of $p_j/p_\infty < 2$ the equation given by Pack[16] which is based on linear theory applies satisfactorily, i.e.

$$\frac{L_j}{d_j} = 2.695\sqrt{\left(\frac{p_j}{p_\infty}\right)^{0.291} - 1.205} . \qquad \text{(II-18)}$$

For higher pressure ratios, purely analytical determinations of the wavelength have been unsuccessful. In Reference 20 an empirically determined equation for the primary wavelength is given by

$$\frac{L_j}{d_j} = 1.52\left(\frac{p_j}{p_\infty}\right)^{0.497} + 1.55\left[(2M_j^2 - 1)^{\frac{1}{2}} - 1\right]$$

$$= 0.55\beta_j + 0.5\left\{\frac{1}{1.55}\left[\left(\frac{p_j}{p_\infty} - 2\right)\beta_j\right]^{\frac{1}{2}} - 1\right\} . \qquad \text{(II-19)}$$

This equation was derived from a large amount of experimental data obtained with high pressure air jets expanding into still air at atmospheric pressure or lower with $p_j/p_\infty > 2$. It was shown in Reference 20 that the jet nozzle exit angle, θ_N, had little effect on the primary wavelength.

1.5 Distance to the First Mach Disc

A method for calculating the distance from the nozzle exit to the first Mach disc, L_{md}, has been given in Reference 25. The assumption is made that the stati. pressure immediately downstream of the Mach disc or normal shock is equal to the ambient pressure of the surroundings, p_∞. Thus if the centerline Mach number and pressure distribution, which are identical up to the shock for any fixed nozzle, are known, the shock position can be computed.

1.6 Jet Mixing Region

A qualitative picture of the mixing regions of the jet exhaust can be obtained by referring to the sketch overleaf. Immediately downstream of the nozzle, an annular mixing region, I, surrounds a core of potential flow. Region III consists of an entirely turbulent mixing zone in which the velocity profiles across the jet are similar. Region II in turn represents a transition zone between the conditions at I and III.

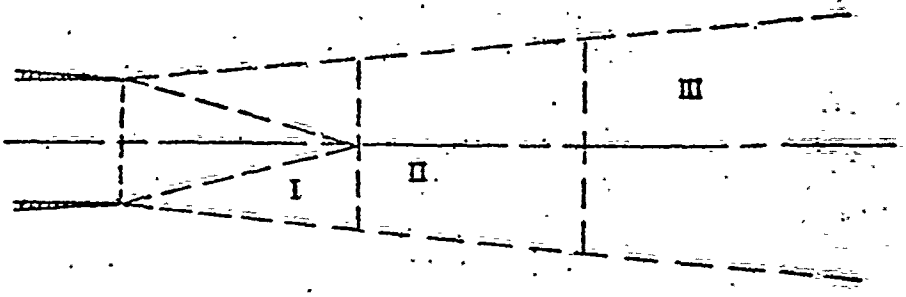

A mean velocity distribution of the flow in the mixing zone of Region III can be obtained by using an error function as the velocity profile. This is given by

$$\frac{u}{u_j} = \frac{1}{2}\left[1 + \operatorname{erf}\left(\sigma \frac{r}{x}\right)\right] \qquad \text{(II-20)}$$

where u_j = the jet free stream velocity

σ = spreading rate parameter

$$\operatorname{erf}\left(\sigma \frac{r}{x}\right) = \frac{2}{\sqrt{\pi}} \int_0^{\sigma \frac{r}{x}} e^{-z^2}\, dz .$$

To account for the compressibility of the jet fluid, Tripp has suggested the following relationship for the spreading rate parameter:

$$\sigma = 12 + 2.758 M_j . \qquad \text{(II-21)}$$

The value of $\sigma = 12$ has been established for the case of incompressible flow. An evaluation of the spreading rate parameter is presented in Reference 39 (see Fig.8) in which Tripp's relationship is shown to underestimate the value of σ above $M_j = 1.8$ and overestimate the value of the parameter below this Mach number.

1.7 Jet Noise

With the increased use of jet aircraft, much more attention is being focused on the problem of jet noise (see Refs.9 and 10). The total radiated acoustic power of a subsonic jet has been shown to correlate with the Lighthill parameter, that is

$$W \sim \frac{\rho_\infty A_j u_j^8}{a_\infty^5} . \qquad \text{(II-22)}$$

An example of such correlation is presented in Figure 9. These results showing the sound power produced by a subsonic jet exhausting into a medium at rest at various jet temperatures were obtained from Reference 41.

For a supersonic jet, attempts have been made to correlate the sound power by adding a suitable factor to the Lighthill parameter to account for the noise generated in the supersonic portion of the jet. These correlations are still not very satisfactory.

2. JETS EXHAUSTING INTO A MOVING STREAM

The generalized flow pattern of an under-expanded axisymmetric jet with an exit nozzle diameter equal to the base diameter exhausting into a stream moving faster than the speed of sound ($M_\infty > 1$) is shown in the sketch below:

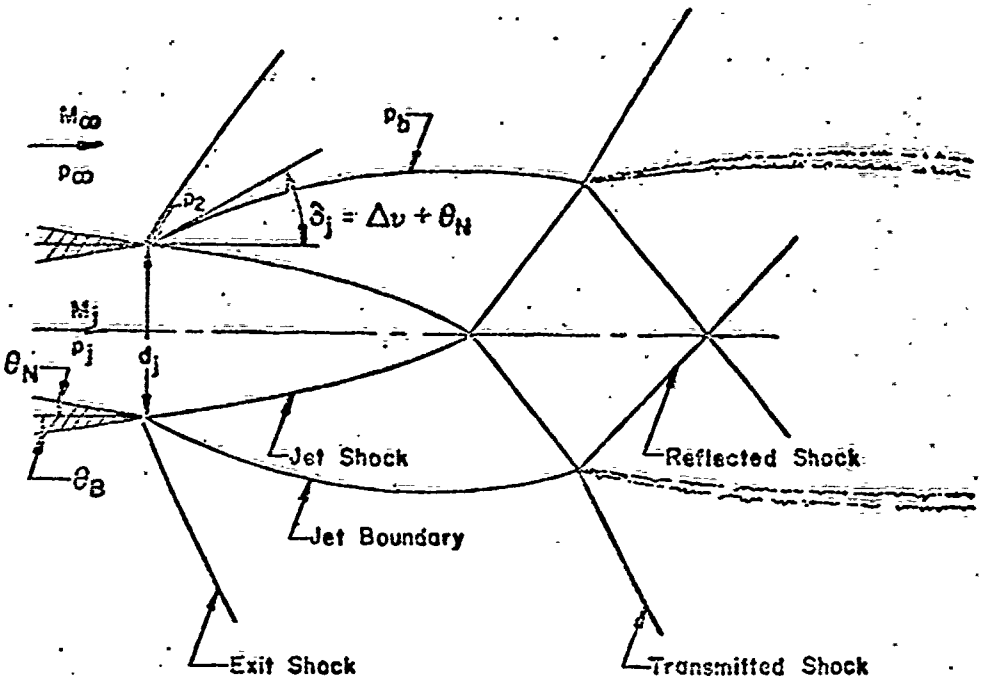

On emerging from the nozzle, the expanding jet sets up a disturbance in the external flow producing an exit shock. The pressure at the jet boundary just aft of the nozzle lip, p_2, is a balance between the external pressure downstream of the shock wave caused by the deflection angle, δ_j, and the jet pressure downstream of the expansion fan through the angle, $\Delta\nu$. The pressure along the jet boundary, p_b, also varies in this case because of the changing slope of the boundary and the three-dimensional flow effects. The jet shock remains in the form of a shock diamond at pressure ratios higher than for the case of the ambient medium because of the increase in pressure at the jet boundary. Depending on the conditions in the two streams the jet shock is partially reflected at the boundary. The periodic structure of the jet is much less defined and in most cases not present at all.

As a first approximation, the flow pattern in the vicinity of a blunt-based body in a moving stream can be considered as a combination of a sharp base jet exhausting into a medium at rest and a moving stream. Up to a streamline separating the moving stream from the quiescent medium in the base region, the flow pattern is similar to that of a jet exhausting into the medium at rest. Beyond this streamline the external flow experiences an exit shock resulting in a flow pattern as described above. The pressure at the base of the model is of course dependent upon the jet and free-stream conditions and should be determined by the methods outlined in Reference 5 when an accurate representation of the flow pattern is desired.

2.1 Initial Inclination of the Jet Boundary

Conditions at the jet boundary immediately downstream of the nozzle exit are depicted in the following sketch:

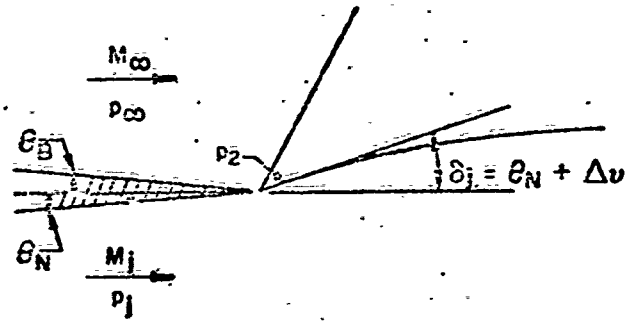

Conditions in the jet or expansive flow are still governed by Equations (II-1), (II-2) and (II-3). For the external or compressive flow, conditions are governed by the following equation:

$$\tan\delta_j = \frac{\left(\frac{p_2}{p_\infty} - 1\right)}{\gamma_\infty M_\infty^2 - \left(\frac{p_2}{p_\infty} - 1\right)}\left[\frac{2\gamma_\infty M_\infty^2 - (\gamma_\infty - 1) - (\gamma_\infty + 1)\frac{p_2}{p_\infty}}{(\gamma_\infty + 1)\frac{p_2}{p_\infty} + (\gamma_\infty - 1)}\right]^{\frac{1}{2}} \qquad \text{(II-23)}$$

which for $\gamma_\infty = 7/5 = 1.4$ reduces to

$$\tan\delta_j = \frac{5\left(\frac{p_2}{p_\infty} - 1\right)}{7M_\infty^2 - 5\left(\frac{p_2}{p_\infty} - 1\right)}\left[\frac{7M_\infty^2 - \left(6\frac{p_2}{p_\infty} + 1\right)}{\left(6\frac{p_2}{p_\infty} + 1\right)}\right]^{\frac{1}{2}} \qquad \text{(II-24)}$$

When $\theta_N = \theta_B = 0$ then $\Delta\nu$ and δ_j must be equal and the conditions existing at the nozzle exit are obtained by equating, for example, Equations (II-6) and (II-24). Such solutions have been obtained for various jet conditions exhausting into a stream at Mach numbers greater than 1.0 with $\gamma_\infty = 1.4$. and $\theta_N = \theta_B = 0$. The results

showing the effects of the various jet and free stream conditions are shown in Figures 10, 11 and 12.

For small values of the angle, δ_j, the ratio of the pressures across the shock in the external flow is given by

$$\frac{p_2}{p_\infty} = 1 + \frac{\gamma_\infty M_\infty^2}{\beta_\infty}\delta_j \qquad \text{(II-25)}$$

or

$$\delta_j = \frac{p_2 - p_\infty}{p_\infty}\frac{\beta_\infty}{\gamma_\infty M_\infty^2} . \qquad \text{(II-26)}$$

To the first order (see Eqn. (II-14)), conditions in the expansive flow are related to $\Delta\nu$ by the expression

$$\Delta\nu = \frac{p_j - p_2}{p_j}\frac{\beta_j}{\gamma_j M_j^2} . \qquad \text{(II-27)}$$

Equating the expressions for δ_j and $\Delta\nu$ gives the following relationship for the conditions existing at the nozzle exit.

$$\frac{p_j - p_2}{p_2 - p_\infty} = \frac{p_j \beta_\infty \gamma_j M_j^2}{p_\infty \beta_j \gamma_\infty M_\infty^2} \qquad \text{(II-28)}$$

2.2 Jet Boundary Shapes

As in the case of a jet expanding into a quiescent medium, the method of characteristics can be used to determine the boundaries for a jet exhausting into a stream moving with $M_\infty > 1$. For a jet expanding into a moving stream, conditions at the boundary cannot be considered under a constant pressure but must be determined by the interaction of the jet and external stream. If the stream flow is hypersonic, the Newtonian approximation can be used to determine the jet boundary pressure. This condition is represented by

$$\frac{p_b}{p_\infty} = \gamma_\infty M_\infty^2 \sin^2\delta_b + 1 . \qquad \text{(II-29)}$$

The results of calculations of jet boundaries using the method of characteristics for the jet flow and the above boundary conditions are presented in Reference 21. Representative boundaries obtained from this Report are reproduced in Figure 13.

An approximate technique employing this same boundary condition is presented in Reference 28. In this method, one-dimensional flow theory in conjunction with Newtonian theory is used to define the jet structure. A comparative boundary with that obtained by the method of characteristics is shown as the dashed curve in Figure 13.

The jet boundaries calculated by each of the above methods represent the dividing streamlines between the jet and the external stream. Comparison with experimental boundaries, which are wide mixing regions are shown by the schlieren photograph in Figure 14 obtained from Reference 29, is therefore rather difficult. In order to obtain a more meaningful comparison, the jet shock boundary can be computed from the jet boundary by a method contained in Reference 28. The method consists of determining the local Mach line at each calculated boundary point for the jet flow. The coalescence of these Mach lines specifies the shock location. The results of such

an analysis as obtained from Reference 29 are shown in Figure 15. The flow field is represented by the photograph and jet boundary shown in Figure 14. As is apparent from the plot, a close approximation between the calculated and experimental jet shock is obtained.

2.3 Jet Mixing Region

For the case of a jet exhausting into a moving stream, the velocity profile in the mixing zone corresponding to Equation (II-19) can be approximated by

$$u = \frac{u_j + u_\infty}{2}\left[1 + \frac{u_j - u_\infty}{u_j + u_\infty}\,\mathrm{erf}\left(\sigma\,\frac{r}{x}\right)\right] \qquad \text{(II-30)}$$

where u_j = the jet free stream velocity
u_∞ = free stream velocity of the moving stream.

The value of σ suggested by Golik[37] is given by

$$\sigma = \frac{12}{1 - \dfrac{u_\infty}{u_j}} + 2.758M_j \qquad \text{(II-31)}$$

where $u_j > u_\infty$.

2.4 Jet Shock Reflection

On the basis of linearized theory, the following parameter was derived in Reference 17 to indicate the strength of the transmitted shock (see sketch on p.9):

$$k = \frac{\gamma_j p_j M_j^2 \beta_\infty}{\gamma_\infty p_\infty M_\infty^2 \beta_j}. \qquad \text{(II-32)}$$

When $k = 1$, the jet shock is not reflected at the jet boundary and no periodic behavior of the jet is noticeable. When the ratio increases or decreases from unity a reflected wave of increasing magnitude occurs. For $k > 1$, the boundary exhibits a periodic behavior.

A similar parameter is derived in Reference 19 and is discussed in Reference 20 as the Kawamura parameter given by

$$\lambda = \frac{1}{\gamma}\sin\mu\cos\mu = \frac{\beta}{\gamma M^2}. \qquad \text{(II-33)}$$

The difference in the value of this parameter between the jet and free stream flows determines the character of the jet shock reflection. If λ_j is larger than λ_∞ (where the values of the parameter are the local values at the interface) a compression wave reflects as a compression wave, while if λ_∞ is larger than λ_j a compression wave reflects as an expansion wave.

III. SCALING PARAMETERS

In ground test facilities, it is many times necessary or more convenient to perform jet tests with test fluids of different composition and with test models of different size from those of the actual vehicle. Thus, it becomes necessary to determine scaling parameters for which the results obtained with the test model are similar to those of the full scale vehicle.

The equations governing the behavior of the interacting jet and free stream flows are at best very approximate. Thus, the use of these equations in deriving similarity parameters is limited. A dimensional analysis of all of the variables involved (see Ref. 2) leads to a host of parameters of which many are relatively unimportant. In what follows, therefore, only those scaling parameters, or more accurately equivalence relationships, are discussed which have been shown or intuitively appear to be important in the simulation of jet exhausts.

In any given problem, only certain scaling parameters are important. For example, when determining the effects of a jet exhaust on base pressure, the parameters governing the shape of the initial portion of the jet are more important than those governing the jet shape far downstream. Thus, an evaluation must be made of the objectives of each specific test in order to determine the extent of simulation required.

3. JET BOUNDARY SIMULATION

In Reference 20 it was shown that, in order to obtain jet boundary simulation, the initial inclination was the most important property that must be duplicated. Simulation of the initial portion of the jet boundary would be important in studies to determine base pressure, base heating, or the effects of the exit shock on adjacent surfaces or jets.

For small turning angles, similarity parameters which provide the same flow turning angle for the model and full scale tests can be obtained starting with Equation (II-14). If a free choice of any of the three variables is allowed, then the first order term of Equation (II-14) indicates that the following relationship between the model and full scale tests must be satisfied to provide identical flow turning angles, $\Delta\omega$:

$$\left[\left(1-\frac{p_\infty}{p_j}\right)\frac{\beta_j}{\gamma_j M_j^2}\right]_m = \left[\left(1-\frac{p_\infty}{p_j}\right)\frac{\beta_j}{\gamma_j M_j^2}\right]_f \qquad \text{(III-1)}$$

If it is assumed as in Reference 46 that the jet Mach number of the model, M_{jm}, is the same as the jet Mach number of the full scale vehicle, M_{jf}, then the following relationship is obtained:

$$\left[\left(1-\frac{p_\infty}{p_j}\right)\frac{1}{\gamma_j}\right]_m = \left[\left(1-\frac{p_\infty}{p_j}\right)\frac{1}{\gamma_j}\right]_f \qquad \text{(III-2)}$$

If instead, it is assumed that the ratio of the static pressure at the nozzle exit to the free stream static pressure is the same for the model and full scale tests, the similarity parameter becomes

$$\left[\frac{\gamma_j M_j^2}{\beta_j}\right]_m = \left[\frac{\gamma_j M_j^2}{\beta_j}\right]_f \quad \text{(III-3)}$$

In Reference 47, this same similarity parameter was obtained by starting with the requirement that the static pressure change caused by a change in flow direction in the jet and external flow must be the same for the model and full scale tests, that is

$$\left[\frac{\Delta p/p}{\delta_j}\right]_m = \left[\frac{\Delta p/p}{\delta_j}\right]_f \quad \text{(III-4)}$$

It was further postulated that since γ_∞ is normally the same for model and full scale tests, M_∞ should also be duplicated. Since γ_j is, however, usually different between model and full scale, M_j of the model would be adjusted according to Equation (III-3) to satisfy the above requirements, that is

$$M_{j_m}^2 = \frac{\gamma_{j_f}}{\gamma_{j_m}} \frac{\beta_{j_m}}{\beta_{j_f}} M_{j_f}^2 \quad \text{(III-5)}$$

The extent to which the constant jet Mach number and the constant jet pressure ratio similarity parameters duplicate the initial inclination angle of the jet can be seen in Figures 16 and 17 respectively. The values of the jet angle for the constant jet Mach number parameter are shown for both a low ($3.72 < p_j/p_\infty < 5.0$) and high ($36.4 < p_j/p_\infty < 53.0$) jet pressure ratio. As is readily apparent, the similarity parameter based on a constant jet pressure ratio gives more nearly equal values of the jet angle than that using a constant jet Mach number.

For the case of a jet exhausting into a moving stream, a similarity parameter can be obtained by starting with Equation (II-28). If the ratios of the static pressures for the model and full scale tests are duplicated the following similarity parameter is obtained:

$$\left[\frac{\beta_\infty \gamma_j M_j^2}{\beta_j \gamma_\infty M_\infty^2}\right]_m = \left[\frac{\beta_\infty \gamma_j M_j^2}{\beta_j \gamma_\infty M_\infty^2}\right]_f \quad \text{(III-6)}$$

Furthermore, if the free stream conditions γ_∞ and M_∞ for the model tests are identical to those in free flight (which is usually the case), the similarity parameter reduces to that given by Equation (III-3) for a jet exhausting into a quiescent medium.

4. JET SHOCK SIMULATION

In some cases it is necessary to duplicate the structure and strength of the shock and expansion waves in the flow field beyond the intersection of the jet shock with

the jet boundary. Such simulation requires the duplication of the parameter given in Equation (II-32). The simulation parameter thus obtained is given by:

$$\left[\frac{p_j \gamma_j M_j^2 \beta_\infty}{p_\infty \gamma_\infty M_\infty^2 \beta_j}\right]_m = \left[\frac{p_j \gamma_j M_j^2 \beta_\infty}{p_\infty \gamma_\infty M_\infty^2 \beta_j}\right]_f \quad \text{(III-7)}$$

Using the assumption that the free stream conditions for γ_∞ and M_∞ for the model tests are identical to those in flight, the parameter reduces to

$$\left[\frac{p_j \gamma_j M_j^2}{p_\infty \beta_j}\right]_m = \left[\frac{p_j \gamma_j M_j^2}{p_\infty \beta_j}\right]_f \quad \text{(III-8)}$$

If the assumption is also made that the model and full scale static pressure ratio is matched, this parameter also reduces to that given by Equation (III-3) or that given by the Kawamura parameter, Equation (II-33).

5. SIMULATION OF JET FLOW PARAMETERS

In this section relationships are defined which govern the simulation of the various jet flow parameters (see Ref.48). The expressions are derived by relating the jet flow parameters to similar free stream parameters.

5.1 Jet Mass Flow

The simulation parameter for the mass flow characteristics is obtained by relating the jet mass flow to a representative free stream mass flow. In equation form,

$$\frac{(\rho u A)_j}{(\rho u A)_\infty} = \frac{p_j M_j \gamma_j^{\frac{1}{2}} (RT)_\infty^{\frac{1}{2}} A_j}{p_\infty M_\infty \gamma_\infty^{\frac{1}{2}} (RT)_j^{\frac{1}{2}} A_\infty} \quad \text{(III-9)}$$

The resulting similarity parameter is therefore

$$\left[\frac{A_j^2 p_j^2 \gamma_j M_j^2 (RT)_\infty}{A_\infty^2 p_\infty^2 \gamma_\infty M_\infty^2 (RT)_j}\right]_m = \left[\frac{A_j^2 p_j^2 \gamma_j M_j^2 (RT)_\infty}{A_\infty^2 p_\infty^2 \gamma_\infty M_\infty^2 (RT)_j}\right]_f \quad \text{(III-10)}$$

In addition to the parameters involved in the simulation of the jet boundary and jet shock, a requirement that $(RT)_j$ of the model be related to that of the full scale engine is obtained.

5.2 Jet Kinetic Energy

Duplication of the kinetic energy per unit mass is obtained by simulation of the velocity ratio of the jet and free streams. In equation form,

$$\frac{u_j^2}{u_\infty^2} = \frac{\gamma_j M_j^2 (RT)_j}{\gamma_\infty M_\infty^2 (RT)_\infty} \quad \text{(III-11)}$$

The resulting similarity parameter becomes

$$\left[\frac{\gamma_j M_j^2 (RT)_j}{\gamma_\infty M_\infty^2 (RT)_\infty}\right]_a = \left[\frac{\gamma_j M_j^2 (RT)_j}{\gamma_\infty M_\infty^2 (RT)_\infty}\right]_f \quad \text{(III-12)}$$

For matched conditions of the free stream parameters, the parameter reduces to

$$\left[\gamma_j M_j^2 (RT)_j\right]_a = \left[\gamma_j M_j^2 (RT)_j\right]_f \quad \text{(III-13)}$$

5.3 Jet Internal Energy

Duplication of the internal energy per unit mass is obtained by simulating the following relationship:

$$\frac{(c_v T)_j}{(c_v T)_\infty} = \frac{(\gamma_\infty - 1)(RT)_j}{(\gamma_j - 1)(RT)_\infty} \quad \text{(III-14)}$$

which gives the following simulation parameter:

$$\left[\frac{(\gamma_\infty - 1)(RT)_j}{(\gamma_j - 1)(RT)_\infty}\right]_a = \left[\frac{(\gamma_\infty - 1)(RT)_j}{(\gamma_j - 1)(RT)_\infty}\right]_f \quad \text{(III-15)}$$

5.4 Jet Enthalpy

Duplication of the enthalpy per unit mass is obtained by simulating the following relationship:

$$\frac{(c_p T)_j}{(c_p T)_\infty} = \left(\frac{\gamma_j}{\gamma_j - 1}\right)\left(\frac{\gamma_\infty - 1}{\gamma_\infty}\right)\frac{(RT)_j}{(RT)_\infty} \quad \text{(III-16)}$$

which gives the following simulation parameter:

$$\left[\frac{(\gamma_\infty - 1)\gamma_j (RT)_j}{(\gamma_j - 1)\gamma_\infty (RT)_\infty}\right]_a = \left[\frac{(\gamma_\infty - 1)\gamma_j (RT)_j}{(\gamma_j - 1)\gamma_\infty (RT)_\infty}\right]_f \quad \text{(III-17)}$$

5.5 Jet Momentum

The simulation parameter for the jet momentum is obtained from the relationship:

$$\frac{(\rho u^2 A)_j}{(\rho u^2 A)_\infty} = \frac{p_j \gamma_j M_j^2 A_j}{p_\infty \gamma_\infty M_\infty^2 A_\infty} \quad \text{(III-18)}$$

giving the similarity parameter:

$$\left[\frac{p_j \gamma_j M_j^2 A_j}{p_\infty \gamma_\infty M_\infty^2 A_\infty}\right]_a = \left[\frac{p_j \gamma_j M_j^2 A_j}{p_\infty \gamma_\infty M_\infty^2 A_\infty}\right]_f \quad \text{(III-19)}$$

5.6 Jet Thrust

The relationship for the simulation of the jet thrust is obtained by starting with the jet thrust coefficient defined by

$$C_F = \frac{F_j}{q_\infty A_\infty} \tag{III-20}$$

where the thrust is given by

$$F_j = (\rho u^2 A)_j + (p_j - p_\infty)A_j \, . \tag{III-21}$$

The simulation parameter thus obtained is given by

$$\left\{\frac{A_j}{\gamma_\infty M_\infty^2 A_\infty}\left[\frac{p_j}{p_\infty}(1 + \gamma_j M_j^2) - 1\right]\right\}_m = \left\{\frac{A_j}{\gamma_\infty M_\infty^2 A_\infty}\left[\frac{p_j}{p_\infty}(1 + \gamma_j M_j^2) - 1\right]\right\}_f \tag{III-22}$$

6. BASE HEATING SIMULATION PARAMETERS

Much experimental and some theoretical work has been done recently on the problems associated with the base heating of rocket-powered models. A general discussion of the important simulation parameters is presented in Reference 49. In addition to those parameters already discussed were the jet emissivity, jet-to-base form factor, engine efficiency, nozzle wall cooling effects, fuel distribution pattern, flame speed and ignition delay characteristics of the entrained fuel and other associated properties.

Similarity parameters concerning the base flow patterns are derived in Reference 47. The resulting relationships are referred to as an excess pumping mass parameter

$$\frac{\Delta V_j}{V_\infty} = \frac{(\rho u)_j}{(\rho u)_\infty}\frac{\pi d_j^2}{A_B}\int_{r_j}^{\infty}\frac{\rho u}{(\rho u)_j}\frac{dr}{d_j} \tag{III-23}$$

and a jet boundary streamline total pressure head parameter

$$\frac{p_t(r_j)}{q_\infty} = \frac{\rho(r_j)[u(r_j)]^2}{\gamma_\infty M_\infty^2 p_\infty} \tag{III-24}$$

where r_j refers to the streamline within which the mass flow is equal to the jet mass flow and the velocity and density profiles are defined by some distribution such as that given by Equation (II-20).

7. JET MIXING SIMULATION

Very little work has been done in the derivation of simulation parameters for the mixing processes along the jet boundary. These processes are governed by the

viscosities, momentums, and heat transfer rates of the local elements of the flow at the jet boundary. It would appear therefore that simulation of the mixing processes would be governed by the degree of simulation of the jet flow parameters discussed in Section III-5.

8. JET NOISE SIMULATION

The simulation parameter for the noise generated in the far field of a subsonic jet and a portion of the supersonic jet can be derived from Equation (II-22). The following parameter is obtained for the correlation of sound power:

$$\left[\rho_\infty A_j \frac{\gamma_j^n u_j^8 (RT)_j^n}{\gamma_\infty^{5/2} (RT)_\infty^{7/2}}\right]_m = \left[\rho_\infty A_j \frac{\gamma_j^n u_j^8 (RT)_j^n}{\gamma_\infty^{5/2} (RT)_j^{7/2}}\right]_f . \qquad \text{(III-25)}$$

For matched conditions of the free stream conditions the parameter reduces to

$$\left[A_j \gamma_j^n u_j^8 (RT)_j^n\right]_m = \left[A_j \gamma_j^n u_j^8 (RT)_j^n\right]_f . \qquad \text{(III-26)}$$

Thus, under these conditions the jet sound power is proportional to the jet kinetic energy.

A summary of the scaling parameters discussed in the preceding paragraphs is presented in Table I. An examination of the general simulation parameters for the various jet characteristics reveals that the pressure ratio function varies appreciably among the relationships. It would appear therefore that a matching of this parameter between model and full scale tests is essential for good simulation. As pointed out previously, the free stream conditions of γ_∞ and M_∞ for the full scale article can be duplicated with relative ease for a model in ground test facilities. If it is further assumed that the other free stream conditions are matched, the simulation parameters reduce to those shown in the second column of Table I. Under these conditions, besides matching the initial inclination angle of the jet exhaust, δ_j, simulation of the parameters $\gamma_j M_j^2/\beta_j$, $\gamma_j M_j^2 A_j$ and $(RT)_j$ between model and full scale tests appears desirable.

As mentioned in the introduction to this section, a complete simulation of all of the parameters listed in Table I is not required for all jet tests. In the following sections, the jet effects are separated into exit effects and downstream effects. Conditions at the base of the model would appear to depend primarily upon the initial shape of the jet at the nozzle exit. Thus duplication of the initial inclination angle of the jet, δ_j, would suffice for base pressure studies. In addition, for base heating (temperature) studies, duplication of the jet temperature would be required. In studies in which model surfaces are located within or near to the jet stream duplication of the jet flow properties would have to be considered. Thus a thorough examination of the test objectives is required in order to specify which simulation parameters must be duplicated.

IV. METHODS OF JET SIMULATION

Various methods are in use for the experimental simulation of an exhaust jet in ground test facilities. These vary in complexity from the use of simple cold gas jets to an almost exact duplication of the full scale jet. The degree of similitude used or required depends on the particular problem under investigation. Some of the techniques which have been employed or proposed are discussed in the following paragraphs.

Approximate values for the properties of turbojet, ramjet, and rocket exhausts are listed in Table II. The ramjet properties are also typical of an after-burning turbojet. As will be discussed in the following sections, the simulation of these properties is the goal of the other media listed in the Table.

9. COLD GAS JETS

The use of a cold gas for the simulation of a jet exhaust has the primary advantage of relative simplicity in set-up and operation. Cold gases are particularly appealing when the simulation of jet temperature is considered of little importance.

9.1 Air

Since high pressure air supplies are most commonly available, the use of cold air has found wide application for jet studies. As seen in Table II, only the value of R is in the same range of the properties of the jet exhausts which must be duplicated.

9.2 Helium

Cold helium has been used in many studies (see Refs.51 to 53) because the high value of its gas constant, R, allows for an almost exact simulation of the value of $(RT)_j$ for a ramjet or afterburning turbojet. As shown in Section III-5, the simulation of $(RT)_j$ is important for the duplication of jet flow parameters. The high value of the ratio of specific heats for cold helium, however, is a prime disadvantage.

9.3 Carbon Dioxide

The value of the ratio of specific heats of carbon dioxide makes its use attractive for a simulation medium. The low value of its gas constant is, however, a disadvantage. This medium was used in the studies reported in Reference 54 at a temperature of 580°R so that its value of γ matched that of a hot jet of burning hydrogen and air at 2600°R.

10. COLD GAS MIXTURES

In the studies reported in Reference 53, a cold mixture of hydrogen and carbon dioxide was used as the jet fluid. The mixture used (.46 H_2 and .54 CO_2) provided a duplication of $(RT)_j$ for the ramjet conditions as did the use of helium. The value of the ratio of specific heats although lower than that of the helium jet, was still however above that required for exact simulation.

The proportions of hydrogen and carbon dioxide required to simulate $(RT)_j$ for a turbojet exhaust were computed and listed in Table II. For a rocket exhaust the value of $(RT)_j$ is almost identical to that of cold hydrogen. In each case, however, the value of γ_j for the simulation fluid is higher than that of the engine exhaust.

In the study reported in Reference 55, it was shown that by the addition of a third gas to hydrogen and carbon dioxide both the $(RT)_j$ and γ_j of a turbojet exhaust could be simulated. For the case cited in Table II, ethane, C_2H_6, was used as the third gas. It was stated in Reference 55 that the upper temperature limit for which complete simulation is possible with a cold ($T_j = 530^\circ R$) gas mixture is on the order of $1650^\circ R$. By heating the mixture somewhat, simulation for higher temperatures could be achieved.

11. HOT GAS JETS

The properties of a jet exhaust can be simulated much more closely with a hot rather than a cold gas stream. However, the complexity in providing a hot gas jet is increased considerably over that of a cold gas jet.

11.1 Hot Air

The properties of a hot air jet at a temperature ($3300^\circ R$) corresponding to that of a ramjet or after-burning turbojet exhaust are shown in Table II. As a result of heating the air, the ratio of specific heats approaches that of the jet exhaust much more closely than does that of a cold air jet giving close simulation of $(RT)_j$ and γ_j.

11.2 Hydrogen and Air

The use of a burning mixture of hydrogen and air was used in the studies reported in References 53 and 54 to duplicate the properties of an after-burning turbojet. Since the resulting jet properties at a temperature of $3300^\circ R$ are typical of those of a ramjet or after-burning turbojet, they were chosen to represent the properties of a ramjet exhaust in Table II.

11.3 Hydrogen Peroxide

The development of a hydrogen peroxide simulator for jet exhaust tests is described in Reference 56. The characteristics of the simulator exhaust using hydrogen peroxide of 30 per cent concentration (10 per cent pure H_2O) are shown in Table II. As pointed out in Reference 56, the system is much simpler and easier to operate than a burning gas. In addition, the products of decomposition, steam and oxygen, are much safer to handle in ground test facilities.

11.4 Turbojet Simulator

A simulation device described in Reference 57 uses a turbojet combustor for the duplication of a jet exhaust. Such a device, frequently employed, burns a mixture of a hydrocarbon fuel and air. The jet properties can be adjusted to closely simulate those of a turbojet or ramjet exhaust.

12. ROCKET MOTOR SIMULATORS

In order to achieve the duplication of the high temperature of a rocket exhaust (see Table II), resort is made to the use of scaled rocket motors for jet simulation. Both solid and liquid propellent engines are used. Results are presented in Reference 58 wherein a liquid propellent rocket engine operating on gaseous oxygen and hydrogen was used. A combination of liquid oxygen and jet engine fuels has also been used successfully.

In References 48 and 59, turbojet exhaust simulators are described wherein solid-propellent rocket motors are used to simulate the exhaust jet. The characteristics of one of these rocket motors, a JATO unit, are shown in Table II.

A number of methods are employed to introduce the simulation fluids into the model. The most widely used method is to mount the model from a side strut and use the inside of the strut to duct the fluids. A second technique wherein high pressure air is ducted through a sting support and discharged in such a way as to duplicate a jet exhaust is described in Reference 60. A similar technique developed for use for short run time at hypervelocities is described in Reference 61. A third method (see Ref.62) which can be used for jet studies utilizes a duct extended through the wind tunnel nozzle from the upstream stilling chamber. The use of a strut or a sting is thus entirely avoided. Such a method is appealing for transonic studies where strut interference problems are especially troublesome. For missile studies, the duct can also be used to simulate the vehicle body.

The recent interest in space exploration has provided a requirement for a low pressure environment for an emerging jet and stimulated the development of such test chambers. Test cells using cryopumping to provide near vacuum conditions are being developed at a rapid rate. Another novel technique (see Ref.63) using an existing wind tunnel utilizes the low pressure environment existing downstream of a blunt base model mounted in a supersonic wind tunnel as the simulated test chamber.

V. EXPERIMENTAL RESULTS

Numerous studies (Refs.3 to 10) have been made to determine the effects of a jet exhaust on base pressure, stability, drag, interference with nearby wings and control surfaces and other aerodynamic and thermodynamic phenomena using the techniques described in the preceding section. However, very few systematic investigations have been undertaken to determine the reliability of these techniques for the particular problems under study. In the following sections, only those data are presented which indicate the sensitivity of the jet flow properties in simulating actual flow conditions.

13. JET EXIT EFFECTS

Jet exit effects are defined as those effects which should be affected little by the mixing process and therefore should be amenable to prediction by inviscid theories and to simulation by parameters derived therefrom.

13.1 Initial Inclination of the Jet Boundary

Prediction of the initial inclination of the jet boundary by the methods described in Section II has been verified by many experimental studies. As an example of such verification, values of the initial inclination angle of a sonic jet exhausting into a stream of air moving at a Mach number of 1.1 are shown in Figure 18 as obtained from Reference 54. In this investigation, made to confirm the procedure of using cold gas jets to simulate a hot gas stream, air at 520°R and carbon dioxide at 580°R (see Table II) were used as the cold jet gases and a burning mixture of hydrogen and air at 2600°R was used for the hot jet gas. The investigation was conducted in the transonic Mach number range at jet pressure ratios up to six.

13.2 Base Pressure

Results of the effect of a jet exhaust on base pressure are shown in Figure 19. These results were obtained from Reference 64 wherein air and carbon dioxide at 540°R were used as the jet media. The dashed curve in the Figure was obtained from the cold air ($\gamma_j = 1.4$) results using the assumption that nozzle conditions which yield the same value of the initial inclination angle of the jet produce the same base pressure. Similar results presented in Reference 65 show that this same adjustment correlates base pressure data obtained from hot and cold air jet tests.

For the studies reported in References 58 and 67, hot and cold flow models were designed based on the similarity parameter given by Equation (III-3). Base pressure measurements in these investigations correlated very well between the hot and cold flow models.

13.3 Exit Shock Position

In References 52 and 53, studies were made to determine to what extent agreement was obtained among various gaseous media in simulating interference effects on a nearby surface. Air, helium, and a mixture of .46 H_2 and .54 CO_2 at 520°R (see Table II) were used as the jet media. The interference produced by the exit shock of the jets was depicted by its effect on the pressure coefficients measured by pressure orifices on the surface as shown in the following sketch:

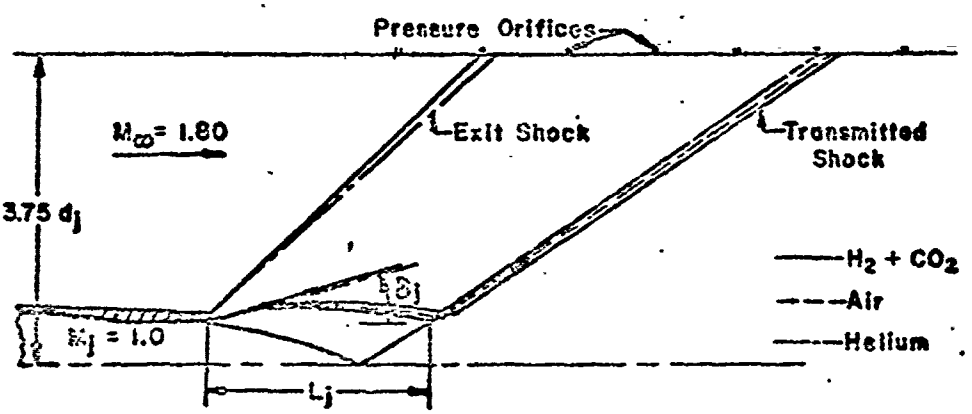

The relative location of the shocks and boundaries were deduced from the pressure data. A typical plot showing the effect of the exit shock on the pressure orifice located 3.47 jet diameters downstream of the jet exit, as obtained from Reference 54, is shown in Figure 20. The dashed curve is obtained from the $\gamma_j = 1.65$ results using the assumption that nozzle conditions which yield the same value of the initial inclination angle of the jet produce the same pressure coefficient.

14. DOWNSTREAM EFFECTS

Jet characteristics which would appear to be affected by the mixing at the jet boundary are considered in the following paragraphs.

14.1 Transmitted Shock Position

In a manner similar to that used to obtain the effects of the exit shock (see sketch in Section V - 13.3), data were also obtained in References 52 and 53 to determine the effects of the transmitted jet shock. A typical plot showing the effects of the transmitted shock on a pressure orifice located 7.63 jet diameters downstream of the jet exit is shown in Figure 21. As the pressure ratio is increased, the shock moves from a position upstream to a position downstream of the pressure orifice because of the increase in the jet primary wavelength, L_j, with a resulting decrease in the pressure coefficient. As shown in Table II, the value of γ_j is identical for the air and $H_2 + CO_2$ mixture, while the value of $(RT)_j$ is essentially the same for the helium and $H_2 + CO_2$ mixtures. By correcting the helium results to a $\gamma_j = 1.40$ to account for the difference in the initial inclination angle of the jet gives good agreement with the $H_2 + CO_2$ results for shock position. Although the initial inclination angles for the air and $H_2 + CO_2$ mixture should be identical, the difference in shock position is probably a result of the difference in mixing caused by the large difference in the value of $(RT)_j$ between these media.

14.2 Transmitted Shock Strength

The difference in the level of the values of the pressure coefficient in Figure 21 before and after the transmitted shock passes over the pressure orifice indicates a difference in the strength of this shock between the helium jet and the air and $H_2 + CO_2$ mixture jets. The ratio of these differences for the case shown is approximately proportional to the ratio of the values of the similarity parameter given by Equation (III-7). In the case of the helium jet the reflected shock (see sketch in Section V - 13.3) is of greater magnitude than that of the $H_2 + CO_2$ and air jets which in turn reduces the strength of the transmitted shock.

14.3 Transmitted Shock Angle

The results of References 51 to 54 for free stream Mach numbers of 1.1 to 2.02 indicate that the angle which the transmitted shock makes with the centerline of the jet is very nearly equal to the Mach angle based on the free stream Mach number. It should be noted, however, that these investigations were limited to jet pressure ratios less than 10.

14.4 Jet Boundary Shape

The relative locations of the jet boundaries for the Reference 53 results shown previously (see sketch in Section V - 13.3) can be deduced from the shock positions. The $H_2 + CO_2$ mixture boundary would be largest, followed by the air and helium boundaries respectively. The fact that the positions of both the jet and the transmitted shock for the helium jet can be made to agree with the positions of these shocks for the $H_2 + CO_2$ mixture by correcting for the difference in the initial inclination angle of the jets, indicates that these boundaries would be identical if compared using the same exit angle conditions. For these jets, the values of $(RT)_j$ are approximately equal. Since γ_j for the $H_2 + CO_2$ mixture and air are the same, the difference in the jet boundary shape is attributed to the difference in $(RT)_j$ between the jets (see Table II).

The results of other investigations (see Refs.68 and 69) also indicate a slight increase in the rate of mixing as the value of $(RT)_j$ is increased.

14.5 Jet Momentum Effects

The importance of simulating the jet momentum is discussed in Reference 62. Results obtained from subsonic tests are presented which indicate that the downwash angle and the drag of an airfoil in the wake of a jet exhaust are both independent of temperature when the momentum is maintained constant.

VI. DISCUSSION

In keeping with the previous Section, the discussion of the results will be separated into the categories of jet exit effects and downstream effects. These categories can also be thought of as those effects which are not affected by jet mixing and those which are affected by mixing.

15. JET EXIT EFFECTS

As pointed out in Reference 20 and discussed in Section II, matching of the initial inclination angle of the jet, δ_j, is the most important requirement in order to duplicate jet exit effects between a model and full scale vehicle. The results of the previous Section and of many investigations show that this angle can be predicted accurately by the Prandtl-Meyer equations for a two-dimensional expansion (see Section II - 1.1).

The results shown previously also indicate that base pressure results and data affected by exit shock position can be correlated among tests conducted with various jet media. These correlations are obtained by assuming that nozzle conditions which give the same initial inclination angle of the jet produce identical results.

No satisfactory similarity parameter has been derived to provide an expression relating all of the parameters which affect the initial inclination angle of a jet. A free choice of these parameters to obtain similarity is proposed, however, by using data such as presented in Figures 1,2,10,11 and 12. Some measure of success in jet flow studies has been achieved by duplicating the jet pressure ratio, P_j/P_∞,

nozzle boat-tail angle, θ_n , and the free stream fluid properties and using the similarity parameter $\gamma_j M_j^2/\beta_j$ given by Equation (III-3) to account for the difference in γ_j of the jet media.

From the foregoing, therefore, it does appear that jet exit effects obtained from model tests can be used with some measure of confidence in predicting full scale results.

16. DOWNSTREAM EFFECTS

The results presented in Section V, although limited in scope, indicate that if the jet inclination angle and $(RT)_j$ are matched the jet boundary shape and the position of the transmitted shock will be duplicated, provided free stream conditions are matched. The strength of the transmitted shock has been shown to be a function of the Kawamura parameter, $\beta_j/\gamma_j M_j^2$. With all other conditions the same, an increase in $(RT)_j$, which represents an increase in jet velocity, produces an increase in the jet boundary.

Although matching of $(RT)_j$ appears to provide a means of simulating the mixing boundary, no correlation parameters are available for use in predicting full scale results from data obtained at unmatched conditions of $(RT)_j$.

When wing or tail surfaces are immersed in or placed near to the jet exhaust, duplication of the jet momentum has been shown to be an important equivalence parameter. Although most of the jet properties such as velocity, temperature and mass flow vary downstream of the jet exit, the jet momentum remains constant and therefore appears to be the most critical jet flow property for simulation.

17. ADDITIONAL REMARKS

From the foregoing it is apparent that although many theoretical and experimental studies have been made to define the jet characteristics, few systematic investigations have been made to determine simulation parameters and the feasibility of various experimental techniques. On the basis of the existing data, the jet pressure ratio is shown to have the greatest effect on performance characteristics. Certain characteristics are affected by conditions in the immediate vicinity of the base. These conditions in turn are shown to be affected most by the initial inclination angle of the jet. Characteristics affected by downstream jet conditions are seen to be dependent upon the parameters, $\gamma_j M_j^2/\beta_j$ and $(RT)_j$ and the jet momentum.

Of the cold gas media listed in Table II, simultaneous duplication of γ_j and $(RT)_j$ is possible only with a 3-component mixture. Use of such a gas would of course allow exact duplication of a jet exhaust without the adjustment of any of the remaining variables according to the scaling parameters. However, tests with such mixtures are required to obtain experimental verification of their use.

Use of the 1- or 2-component cold gas media does require an adjustment of other variables to account for the lack of duplication of both γ_j and $(RT)_j$. One possible combination which would satisfy the most critical simulation parameters is to use the

following procedure. Initially select a gas which duplicates $(RT)_j$ and furthermore specify model operation at matched jet pressure ratios, p_j/p_∞. Assuming γ_j is not matched, an adjustment is made in u_j of the model to satisfy the parameter $\gamma_j u_j^2/\beta_j$ to account for duplication of the jet shock properties. Since, as shown in Figure 17, this correction does not completely provide the necessary correction to the flow turning angle of the jet, $\Delta\nu$, the nozzle exit angle can be adjusted according to Equation (II-13) to provide duplication of the initial inclination angle, δ_j, of the jet. Simulation of the remaining important scaling parameter, the jet momentum, is obtained by an adjustment of the model exit area according to Equation (III-19).

VII. REFERENCES AND BIBLIOGRAPHY

Section I

1. Squire, H.B. — *Jet Flow and Its Effects on Aircraft.* Aircraft Eng., Vol.XXII, No.253, March 1950, p.62.

2. Li, T.Y. et alii — *The Design of Wind Tunnel Experiments for the Study of Jet-On Effects.* NAVORD Report 3473, April 1953.

3. Krzywoblocki, M.Z. — *Jets - Review of Literature.* Jet Propulsion, Vol.26, No.9, September 1956, p.760.

4. Behelm, M.A. et alii — *Jet Effects on Annular Base Pressure and Temperature in a Supersonic Stream.* NASA TR R-125, 1962.

5. Chow, W.L. — *On the Base Pressure Resulting from the Interaction of a Supersonic External Stream with a Sonic or Subsonic Jet.* Journal of the Aerospace Sciences, Vol.25, No.3, March 1959, p.176.

6. Hinson, W.F. Falanga, R.A. — *Effect of Jet Pluming on the Static Stability of Cone-Cylinder-Flare Configurations at a Mach Number of 9.65.* NASA TN D-1352, September 1962.

7. Heyman, L.O., Jr. McDearmon, R.W. — *Jet Effects on Cylindrical Afterbodies Housing Sonic and Supersonic Nozzles which Exhaust Against a Supersonic Stream at Angles of Attack from 90° to 180°.* NASA TN D-1016, March 1962.

8. Jackson, B.G. Crabill, N.L. — *Free-Flight Investigation of Jet Effects at Low Supersonic Mach Numbers on a Fighter-Type Configuration Employing a Tail-Boom Assembly.* NACA RM L57F19, August 1957.

9. Hamitt, A.G. — *The Oscillation and Noise of an Overpressure Sonic Jet.* Journal of the Aerospace Sciences, Vol.28, No.9, September 1961, p.673.

10. Howes, W.L. — *Similarity of Far Noise Fields of Jets.* NASA TR R-52. 1959.

Section II

11. Pai, Shih-I. — *Fluid Dynamics of Jets.* D. van Nostrand Company, Inc., 1954.

12. Ward, G.N. — *Linearized Theory of Steady High-Speed Flow.* Cambridge University Press, 1955, Chap.8.

13. Englert, G.A. — *Operational Method of Determining Initial Contour of and Pressure Field About a Supersonic Jet.* NASA TN D-279. April 1960.

14. Pistolesi, E. Marini, M. — *Linearized Supersonic Flow in an Axisymmetric Jet Issuing in Air at Rest.* Institute of Aeronautics, University of Pisa, TR-1, March 1961.

15. Pistolesi, E. Marini, M. — *Linearized Supersonic Flow of an Axisymmetric Jet in a Supersonic Stream.* Institute of Aeronautics, University of Pisa, TR-2, March 1962.

16. Pack, D.C. — *The Oscillations of a Supersonic Gas Jet Embedded in a Supersonic Stream.* Journal of the Aeronautical Sciences, Vol.23, No.8, August 1955, p.747.

17. Ehlers, F.E. Strand, T. — *The Flow of a Supersonic Jet in a Supersonic Stream at an Angle of Attack.* Journal of the Aerospace Sciences, Vol.25, No.8, August 1958, p.497.

18. Mahoney, J.J. — *The Internal Flow Problem in Axi-Symmetric Supersonic Flow.* Philosophical Transactions of the Royal Society, Series A, Vol.251, 1959, p.1.

19. Kawamura, R. — *Reflection of a Wave at an Interface of Supersonic Flows and Wave Patterns in a Supersonic Compound Jet.* Journal of the Physical Society of Japan, Vol.7, No.5, September-October 1952.

20. Love, E.S. et alii — *Experimental and Theoretical Studies of Axisymmetric Free Jets.* NASA TR R-6, 1959. Supersedes NACA RM L54L31, RM L55J14, RM L56G18, and TN 4185.

21. Hang, C.J. Peterson, J.B. — *Spreading of Supersonic Jets from Axially Symmetric Nozzles.* Jet Propulsion, Vol.28, No.5, May 1958, p.321.

22. Sims, J.L. — *Results of the Computations of Supersonic Flow Fields Aft of Circular Cylindrical Bodies of Revolution by the Method of Characteristics.* ABMA Rep. No.DA-R-49, March 1958.

23. Roe, M. Troesch, B.A. — *Jet Flow with Shocks.* ARS Journal. Vol.30. May 1960. p.487.

24. Love, E.S. — *An Approximation of the Boundary of a Supersonic Axisymmetric Jet Exhausting into a Supersonic Stream.* Journal of the Aeronautical Sciences, Vol.25, No.2. February 1958, p.130.

25. Adamson, T.C., Jr. Nicholls, J.A. — *On the Structure of Jets from Highly Underexpanded Nozzles into Still Air.* Journal of the Aerospace Sciences, Vol.26, No.1. January 1959, p.16.

26. Lord, W.T. — *On Axisymmetrical Gas Jets, with Application to Rocket Jet Flow Fields at High Altitudes.* RAE Report No. Aero 2526. July 1959.

27. Latvala, E.K. Anderson, T.P. — *Studies of the Spreading of Rocket Exhaust Jets at High Altitudes.* Ballistic Missiles and Space Technology, Vol.11, Pergamon Press, 1961.

28. Adamson, T.C., Jr. — *Approximate Methods for Calculating the Structure of Jets from Highly Underexpanded Nozzles.* Institute of Science and Technology, University of Michigan, 3765-26-T. June 1961.

29. Henson, J.R. Robertson, J.E. — *Methods of Approximating Inviscid Jet Boundaries for Highly Underexpanded Supersonic Nozzles.* AEDC-TDR-62-7. May 1962.

30. Chrisman, C.C. — *Evaluation of the Free Jet Spreading Rate Parameters for Axi-Symmetric Flow of Air at Mach Number Three.* Oklahoma State University Thesis, August 1962.

31. Pai, S.I. — *Laminar Jet Mixing of Two Compressible Fluids with Heat Release.* Journal of the Aeronautical Sciences, Vol.23, No.11, November 1956, p.1012.

32. Kleinstein, G. — *An Approximate Solution for the Axisymmetric Jet of a Laminar Compressible Fluid.* Quarterly of Applied Mathematics, Vol.XX, No.1, April 1962, p.49.

33. Vasilin, J. — *Turbulent Mixing of a Rocket Exhaust Jet with a Supersonic Stream Including Chemical Reactions.* Journal of the Aerospace Sciences, Vol.29, No.1, January 1962, p.19.

34. Szablewski, W. — *Turbulente Ausbreitung runden Heissluftstrahles in Bewegter Luft.* Ingenieur-Archiv, XXVI, Band 1958, p.358.

35. Szablewski, W. — *Turbulente Ausbreitung eines runden Heissluftstrahles in ruhender Aussenluft.* Ingenieur-Archiv, XXX, Band 1961, p.95.

36. Pozzi, A. — *Efflusso di un Getto in un Ambiente in Moto.* Missili, Vol.3, February 1961, p.21.

37. Chow, W.L. Korst, H.H. — *On the Flow Structure Within a Constant Pressure Compressible Turbulent Jet-Mixing Region.* Engineering Experimental Station, University of Illinois, ME-TN-393-1, July 1962.

38. Maczynski, J.F.J. — *A Round Jet in an Ambient Co-Axial Stream.* Journal of Fluid Mechanics, Vol.13, Part 4, August 1962.

39. Ryhming, I.L. — *On the Mixing Problem of an Axi-Symmetric Free Jet into Air Including Chemical Reactions.* General Dynamics Corp., Convair Div., ZA-332, March 1961.

40. Johannesen, N.H. — *Further Results on the Mixing of Free Axially Symmetrical Jets of Mach Number 1.40.* ARC 20,981, FM 2817, N.88, May 1959.

41. Rollin, V.G. — *Effect of Jet Temperature on Jet-Noise Generation.* NACA TN 4217, March 1958.

42. Willis, D.R. Glassman, I. — *The Mixing of Unbounded Coaxial Compressible Streams.* Jet Propulsion, Vol.27, December 1957, p.1241.

43. Rousso, M.D. Baughman, L.E. — *Spreading Characteristics of a Jet Expanding from Choked Nozzles at Mach 1.91.* NACA TN 3836, December 1956.

44. Seddon, J. Haverty, L. — *Spread of Velocity in a Cold Jet Discharging with Excess Pressure from a Sonic Exit into Still Air.* RAE TN Aero 2400, November 1955.

45. Eastman, D.W. Radtke, L.P. — *Flow Field of an Exhaust Plume Impinging on a Simulated Lunar Surface.* AIAA Journal, Vol.1, No.6, June 1963, p.1430.

Section III

46. Covert, E.E. — *Jet Simulation in the Wind Tunnel.* Massachusetts Institute of Technology, Naval Supersonic Laboratory, TR 252, July 1957.

47. Goethert, B.H. Barnes, L.T. — *Some Studies of the Flow Pattern at the Base of Missiles with Rocket Exhaust Jets.* AEDC-TR-58-12, June 1950.

48. de Moraes, C.A. et alii — *Design and Evaluation of a Turbojet Exhaust Simulator, Utilizing a Solid-Propellent Rocket Motor, for Use in Free-Flight Aerodynamic Research Models.* NACA RM L54I15, December 17, 1954.

49. Beheim, M.A.
Obery, L.J.
Wind Tunnel Studies of Booster Base Heating. IAS Paper No.62-166, June 1962.

50. Ericsson, L.E.
Scaling Parameters for Simulation of Base Flow Recirculation on Missiles with Multiple Rocket Exhaust Jets. Lockheed Aircraft Corp. M.&S. Div., LMSD 800239, October 1960.

Section IV

51. Bressette, E.
Investigation of the Jet Effects on a Flat Surface Downstream of the Exit of a Simulated Turbojet Nacelle at a Free-Stream Mach Number of 2.02. NACA RM L54E05a, June 23, 1954.

52. Bressette, E.
Leiss, A.
Investigation of Jet Effects on a Flat Surface Downstream of the Exit of a Simulated Turbojet Nacelle at a Free-Stream Mach Number of 1.39. NACA RM L55L13, April 2, 1956.

53. Bressette, E.
Some Experiments Relating to the Problem of Simulation of Hot Jet Engines in Studies of Jet Effects on Adjacent Surfaces at a Free-Stream Mach Number of 1.80. NACA RM L56E07, July 11, 1956.

54. Lee, G.
An Investigation of Transonic Flow Fields Surrounding Hot and Cold Sonic Jets. NASA TN D-853, April 1961.

55. Tempelmeyer, K.E.
An Analytical Study of Hot Jet Simulation with a Cold Gas Mixture. AEDC-TN-58-54, September 1958.

56. Runckel, J.F.
Swihart, J.M.
A Hydrogen Peroxide Hot-Jet Simulator for Wind-Tunnel Tests of Turbojet-Exit Models. NASA Memo 1-10-59L, February 1959.

57. Evans, A.J.
The Simulation of the Effects of Internal Flow in Wind Tunnel Model Tests of Turbojet Powered Aircraft. AGARD AG 19/P9, Papers Presented at the Seventh Meeting of the Wind Tunnel and Model Testing Panel, June 1955, p.53.

58. Herstine, G.L.
et alii
Base Heating Experimental Progress for Saturn S-IV Stage. S.M.F. Fund Paper No. FF-31, Presented at the IAS 30th Annual Meeting, New York, January 22-24, 1962.

59. Leiss, A.
Design and Evaluation of a Turbojet-Exhaust Simulator with a Solid-Propellent Rocket Motor for Free-Flight Research. NACA RM L57E10a, July 5, 1957.

60. Englert, G.W.
Luidens, R.W.
Wind-Tunnel Technique for Simultaneous Simulation of External Flow Field about Nacelle Inlet and Exit Airstreams at Supersonic Speeds. NACA TN 3851, Jan. 1957.

61. Stalmach, C.J.
Cooksey, J.M.
New Test Techniques for a Hypervelocity Wind Tunnel. Aerospace Engineering, Vol.21, No.3, March 1962, p.62.

62. Seddon, J.
Nicholson, L.P.
The Representation of Engine Airflow in Wind Tunnel Model Testing. AGARD AG 19/P9. Papers presented at the Seventh Meeting of the Wind Tunnel and Model Testing Panel, June 1955, p.1.

63. Stitt, L.E.
Interaction of Highly Underexpanded Jets with Simulated Lunar Surfaces. NASA TN D-1095, December 1961.

Section V

64. Palanga, R.A.
et alii
Exploratory Tests of the Effects of Jet Plumes on the Flow Over Cone-Cylinder-Flare Bodies. NASA TN D-1000, February 1962.

65. Baughman, L.E.
Kochendorfer, F.D.
Jet Effects on Base Pressures of Conical Afterbodies at Mach 1.91 and 3.12. NACA RM E57E06, August, 1957.

66. Cortright, E.M., Jr.
Kochendorfer, F.D.
Jet Effects on Flow Over Afterbodies in Supersonic Stream. NACA RM E53H23, November 1953.

67. Goethert, B.H.
Base Flow Characteristics of Missiles with Cluster-Rocket Exhausts. Aerospace Engineering, Vol.20, No.3, March 1961, p.28.

68. Tatro, R.E.
The Spreading Characteristics of Choked Jets Exhausting into a Supersonic Stream. AEDC-TR-55-2, October 1955.

69. Rousso, M.D.
Kochendorfer, F.D.
Experimental Investigation of Spreading Characteristics of Choked Jets Expanding into Quiescent Air. NACA RM E50E03a, August 9, 1950.

TABLE I

Summary of Scaling Parameters

Jet Characteristic	*General Simulation Parameter*	*Simulation Parameter for Matched Stream Conditions and Jet Pressure Ratio*
Boundary in Quiescent Medium	$\left(1 - \frac{p_\infty}{p_j}\right)\frac{\beta_j}{\gamma_j M_j^2}$	$\frac{\gamma_j M_j^2}{\beta_j}$
Boundary in Moving Stream	$\left(\frac{p_j - p_2}{p_2 - p_\infty}\right)\frac{p_\infty \beta_j \gamma_\infty M_\infty^2}{p_j \beta_\infty \gamma_j M_j^2}$	$\frac{\gamma_j M_j^2}{\beta_j}$
Transmitted Shock	$\frac{p_j \gamma_j M_j^2 \beta_\infty}{p_\infty \gamma_\infty M_\infty^2 \beta_j}$	$\frac{\gamma_j M_j^2}{\beta_j}$
Mass Flow	$\frac{p_j^2 \gamma_j M_j^2 (RT)_\infty A_j^2}{p_\infty^2 \gamma_\infty M_\infty^2 (RT)_j A_\infty^2}$	$\frac{\gamma_j M_j^2 A_j^2}{(RT)_j}$
Kinetic Energy	$\frac{\gamma_j M_j^2 (RT)_j}{\gamma_\infty M_\infty^2 (RT)_\infty}$	$\gamma_j M_j^2 (RT)_j$
Internal Energy	$\frac{(\gamma_\infty - 1)(RT)_j}{(\gamma_j - 1)(RT)_\infty}$	$\frac{(RT)_j}{\gamma_j - 1}$
Enthalpy	$\frac{(\gamma_\infty - 1)\gamma_j (RT)_j}{(\gamma_j - 1)\gamma_\infty (RT)_\infty}$	$\frac{\gamma_j}{\gamma_j - 1}(RT)_j$
Momentum	$\frac{p_j \gamma_j M_j^2 A_j}{p_\infty \gamma_\infty M_\infty^2 A_\infty}$	$\gamma_j M_j^2 A_j$
Thrust	$\frac{A_j}{A_\infty \gamma_\infty M_\infty^2}\left[\frac{p_j}{p_\infty}(1 + \gamma_j M_j^2) - 1\right]$	$\gamma_j M_j^2 A_j$
Sound Power	$p_\infty A_j \frac{\gamma_j^4 M_j^8 (RT)_j^4}{\gamma_\infty^{1/2}(RT)_\infty^{7/2}}$	$A_j \gamma_j^4 M_j^8 (RT)_j^4$

TABLE II

Properties of Gaseous Media

Medium	T °R	γ	R *ft-lbf/lb °R*	RT *ft-lbf/lb*
Turbojet Exhaust	1450	1.34	53.0	77,000
Ramjet Exhaust	3300	1.27	59.0	195,000
Rocket Exhaust	5700	1.23	70.0	399,000
Air	520	1.40	53.3	27,700
Helium	520	1.66	386.0	200,000
Hydrogen	520	1.40	768.0	400,000
Carbon Dioxide	520	1.28	35.0	18,200
Carbon Dioxide	580	1.29	35.2	20,400
.15 H_2 + .85 CO_2	520	1.38	148.0	77,000
.46 H_2 + .54 CO_2	520	1.40	374.0	195,000
.14 H_2 + .29 CO_2 + .57 C_2H_6	530	1.34	147.0	78,000
Air	3300	1.30	56.0	185,000
H_2 + Air (burning)	2600	1.29	57.0	148,000
H_2 + Air (burning)	3300	1.27	59.0	195,000
H_2O_2 (.10 H_2O)	1825	1.27	69.9	127,500
JATO	3420	1.27	71.6	245,000
LOX + JP	5880	1.24	70.0	411,000

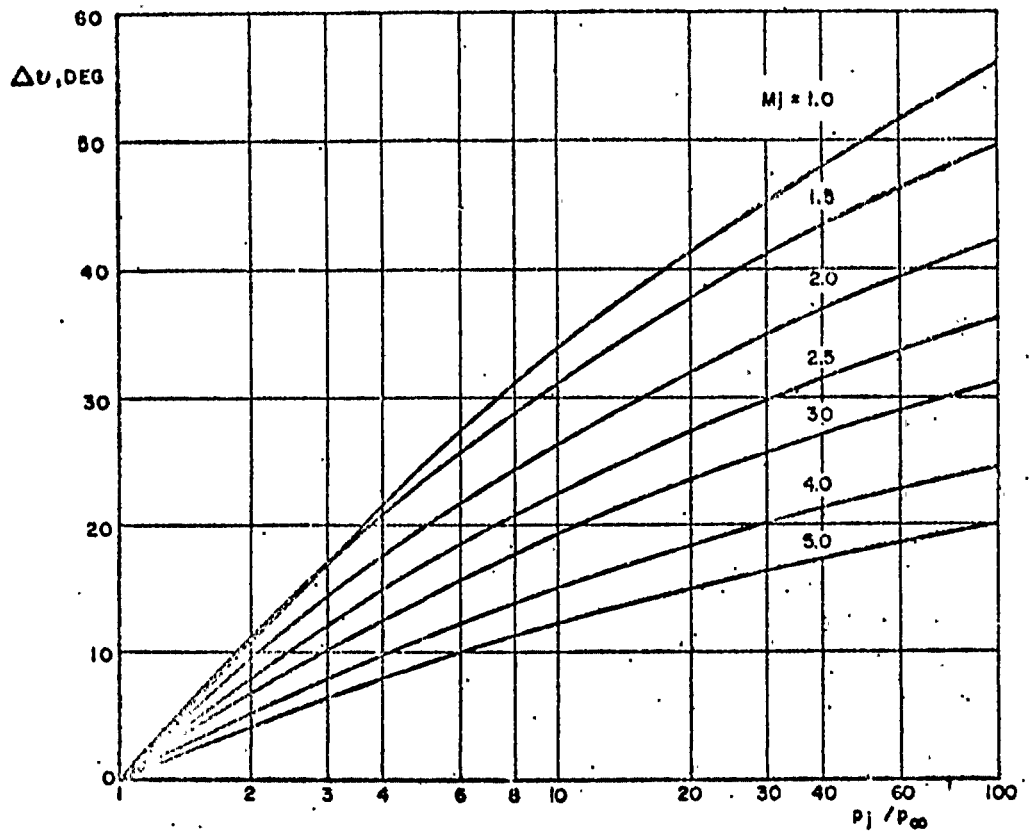

(a) $\gamma_j = 1.667$

Fig.1 Effect of jet Mach number on the initial inclination angle of a jet exhausting into a medium at rest

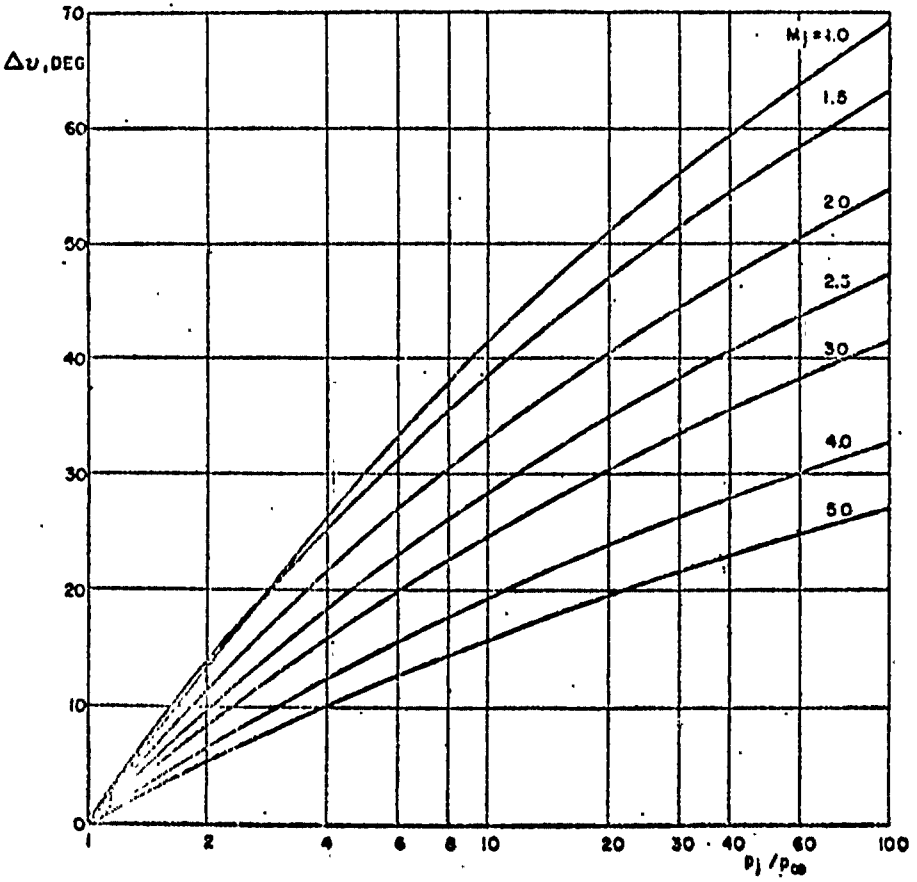

(b) γ_j = 1.38

Fig.1 Continued

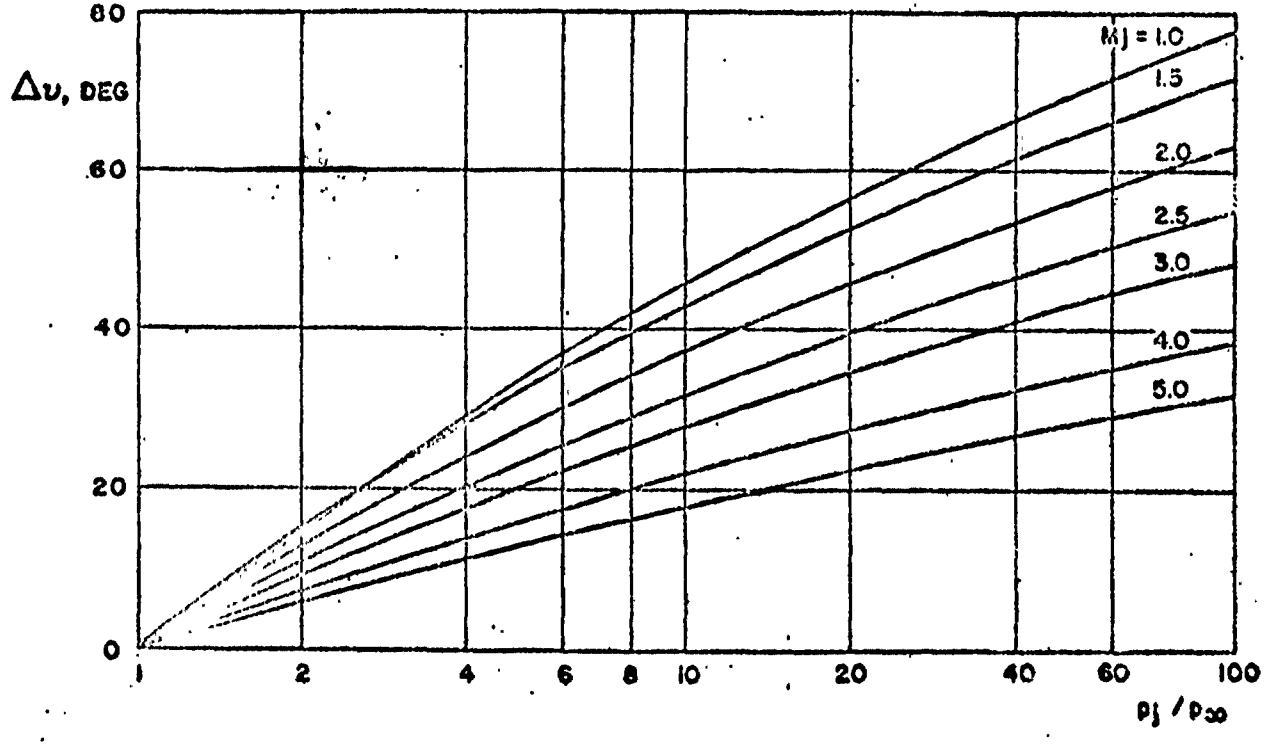

(c) $\gamma_j = 1.25$

Fig.1 Continued

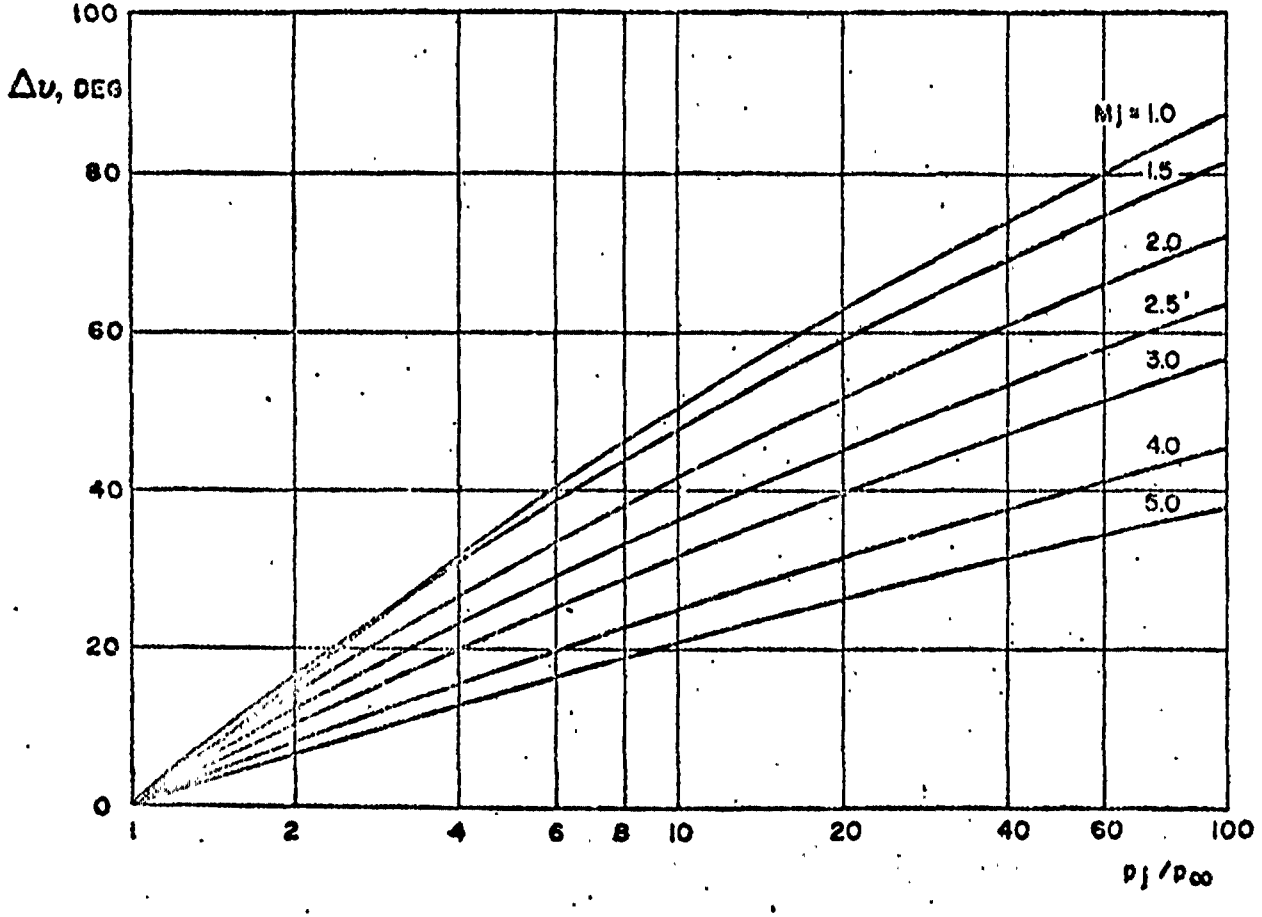

(d) $\gamma_j = 1.133$

Fig.1 Concluded

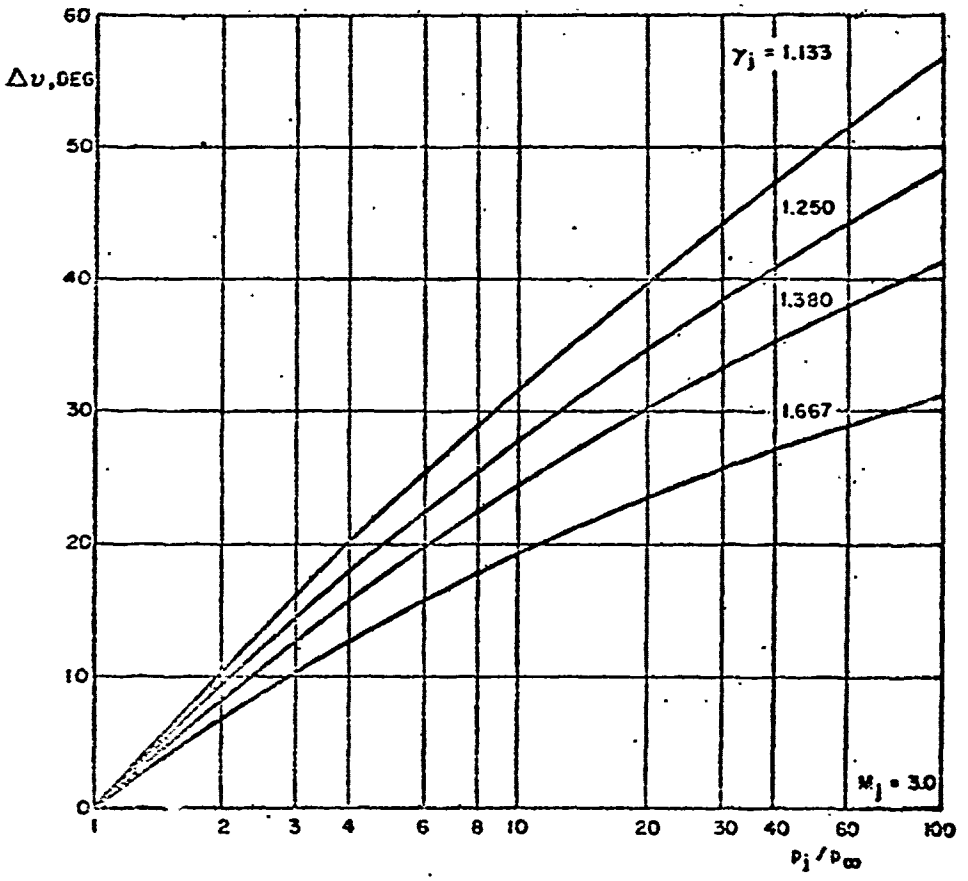

Fig.2 Effect of the ratio of specific heats of the jet on the initial inclination angle of a jet exhausting into a medium at rest

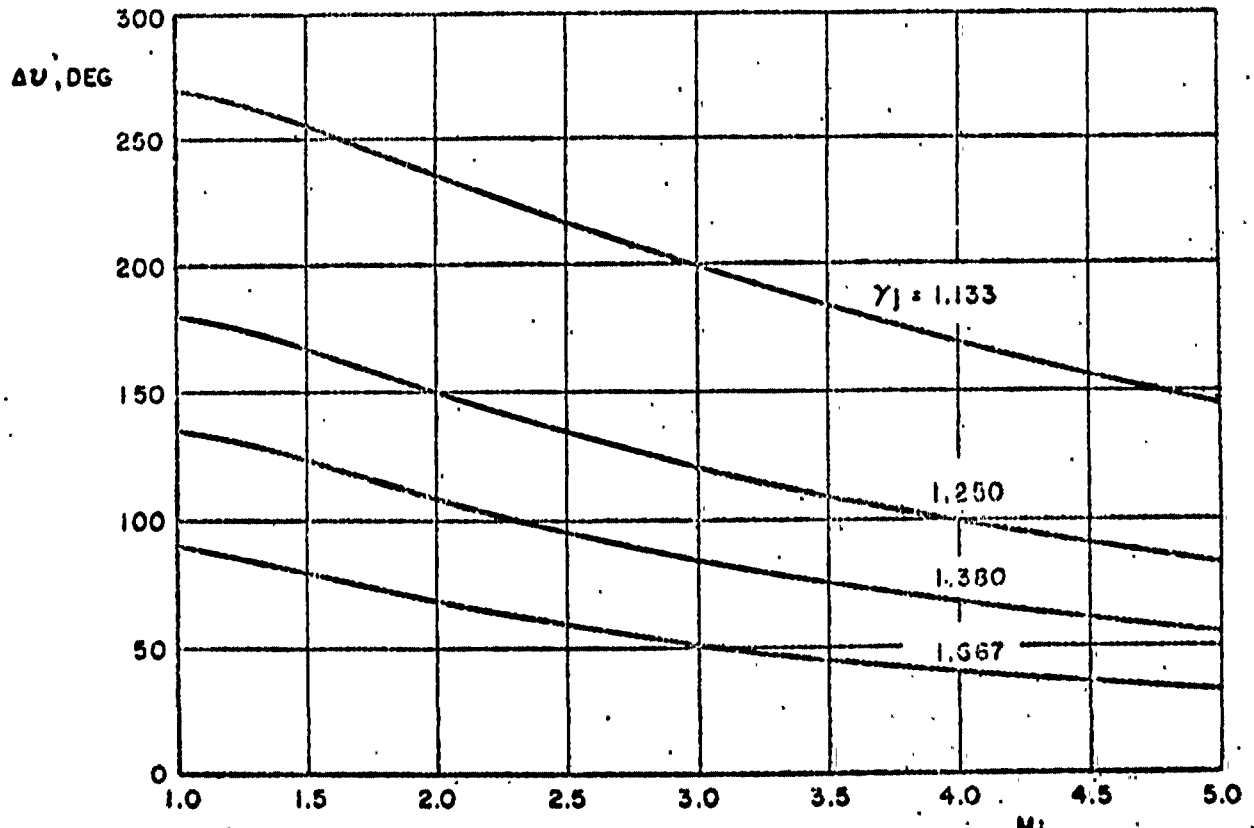

Fig.3 Effect of the ratio of specific heats of the jet on the initial inclination angle of a jet exhausting into a vacuum

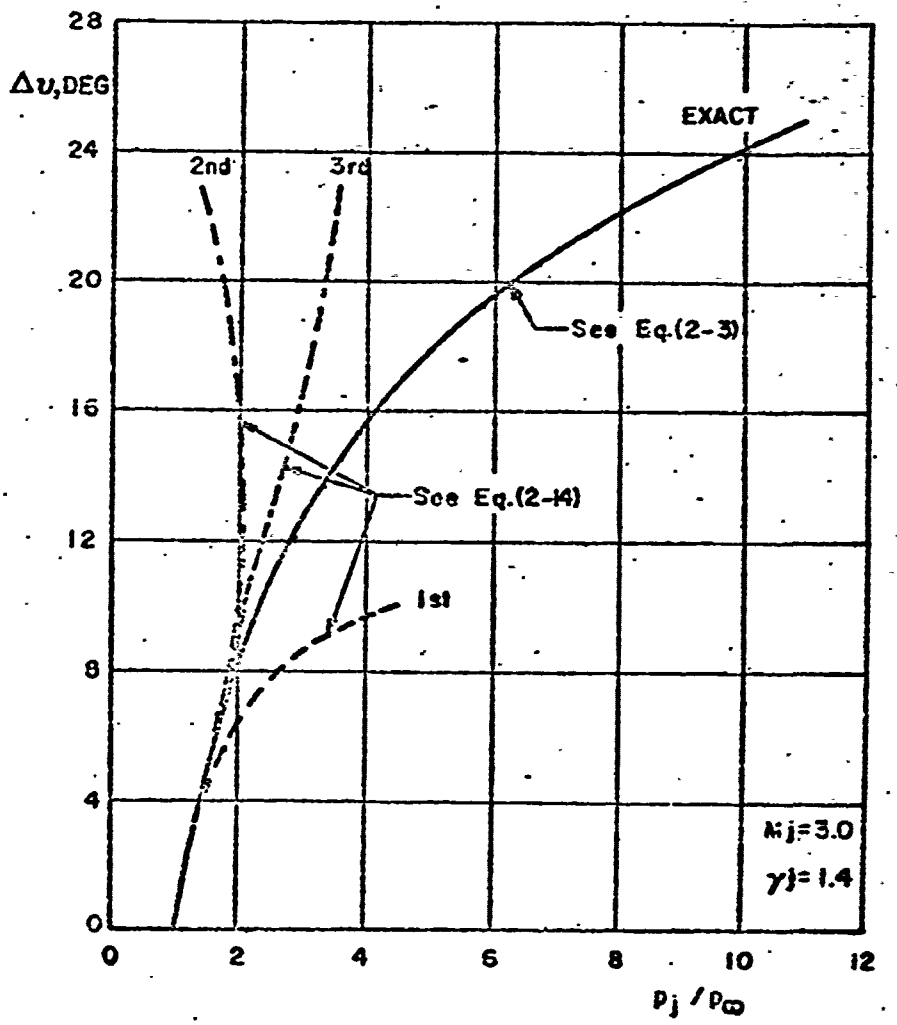

Fig.4 Comparison of initial inclination angle of a jet exhausting into a medium at rest calculated by an exact and an approximate series solution

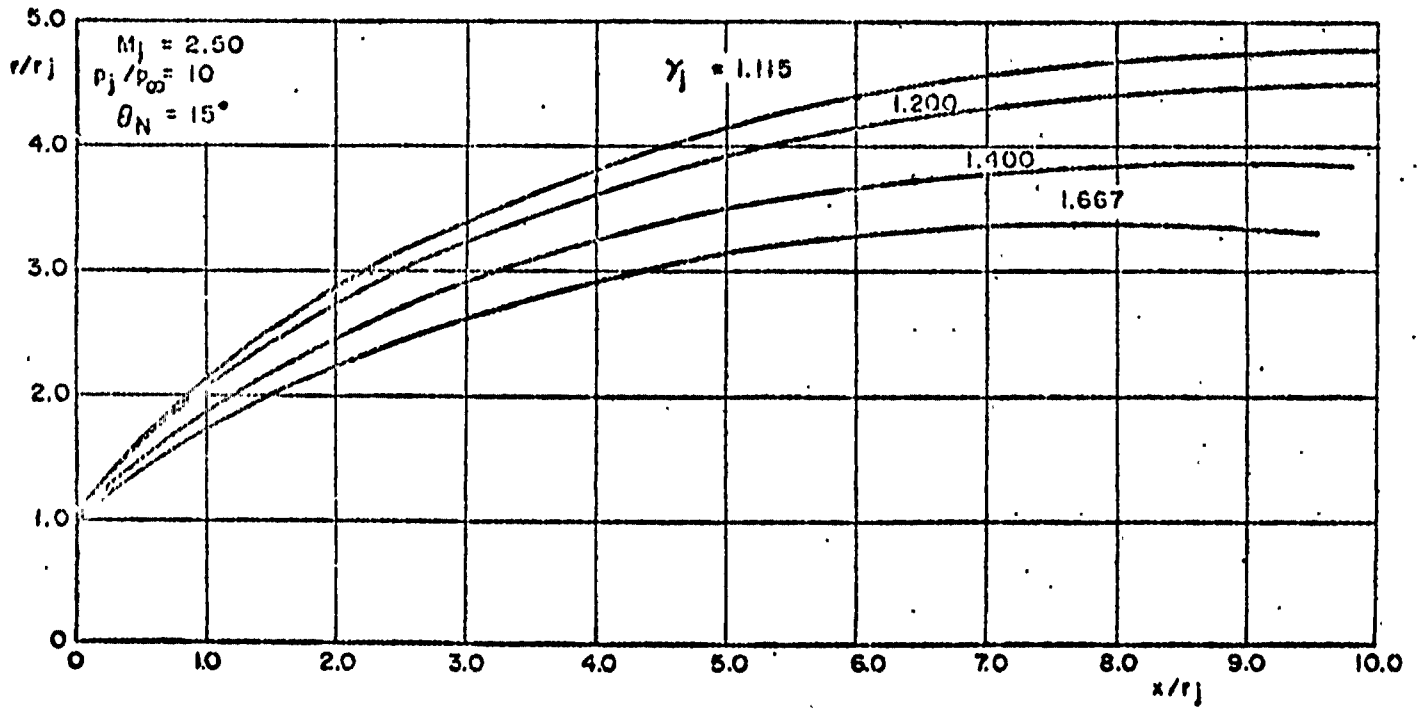

Fig.5 Effect of the ratio of specific heats of the jet on the boundary of a jet exhausting into a medium at rest

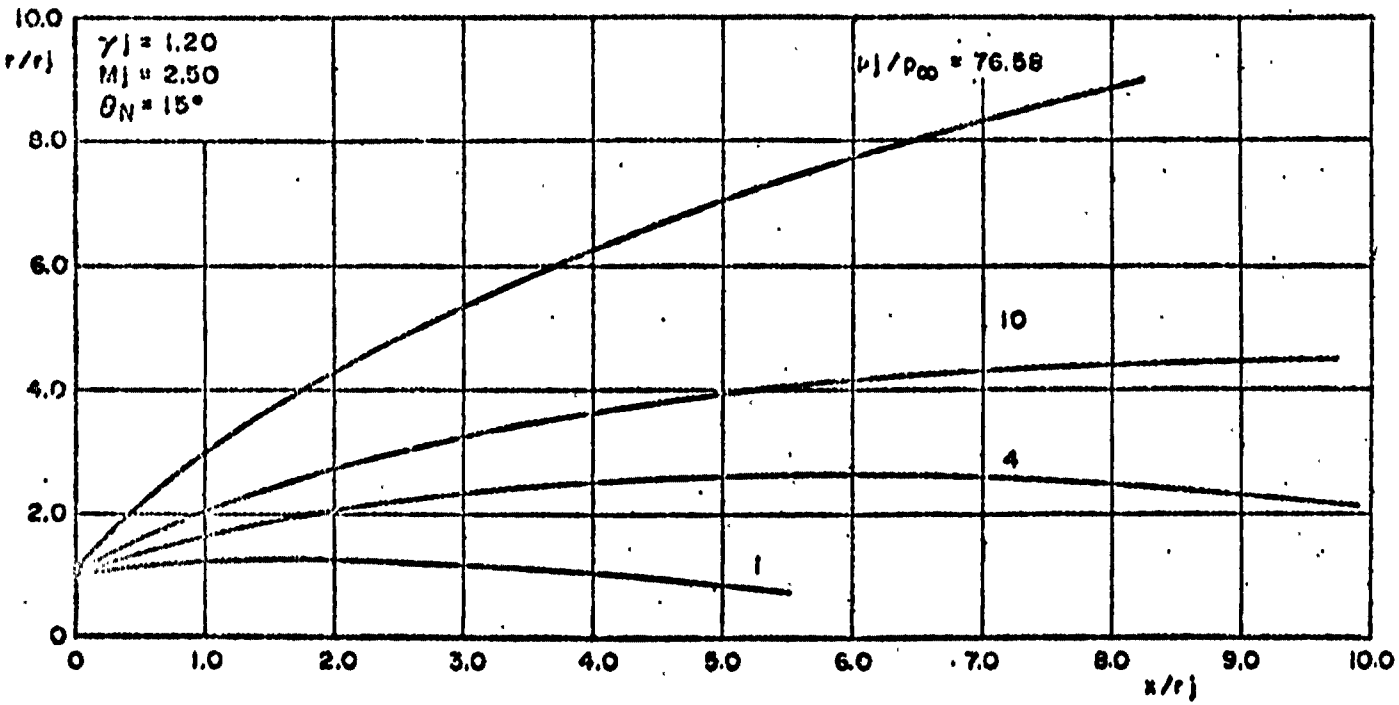

Fig.6 Effect of the jet pressure ratio on the boundary of a jet exhausting into a medium at rest

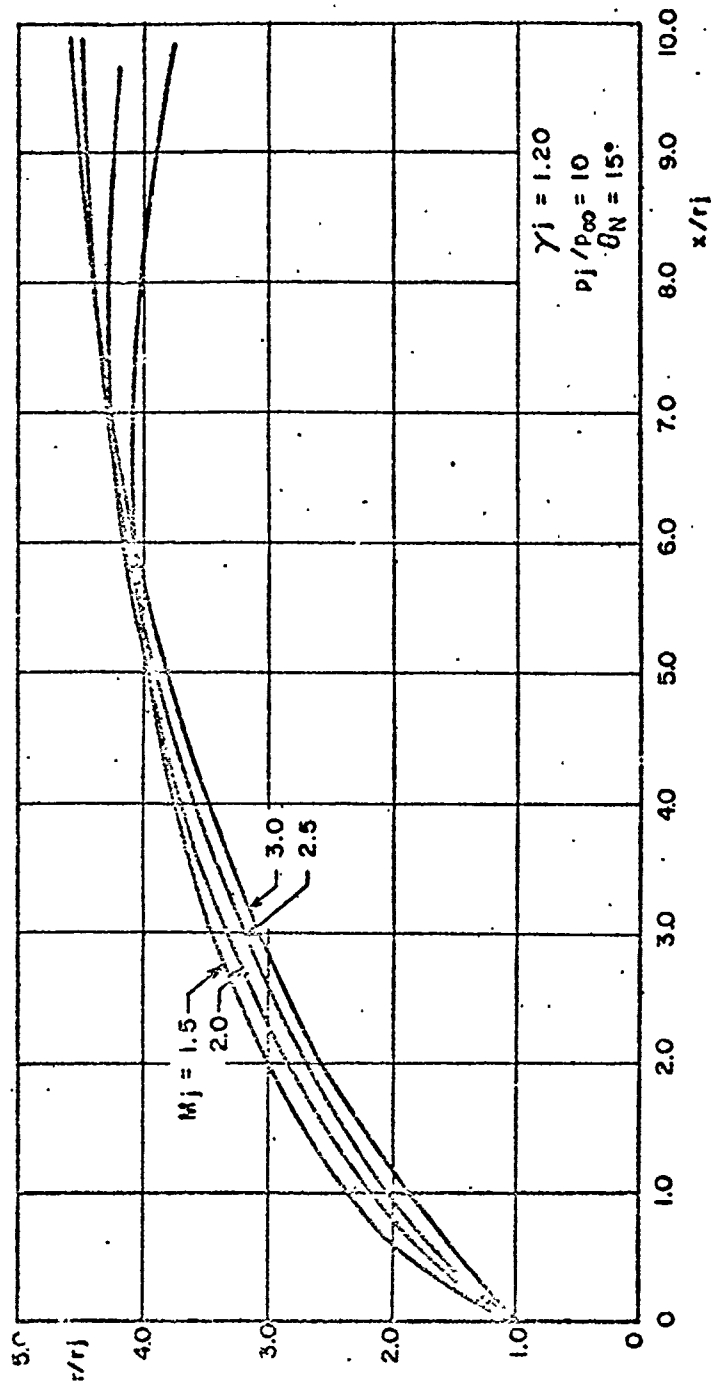

Fig.7 Effect of jet Mach number on the boundary of a jet exhausting into a medium at rest

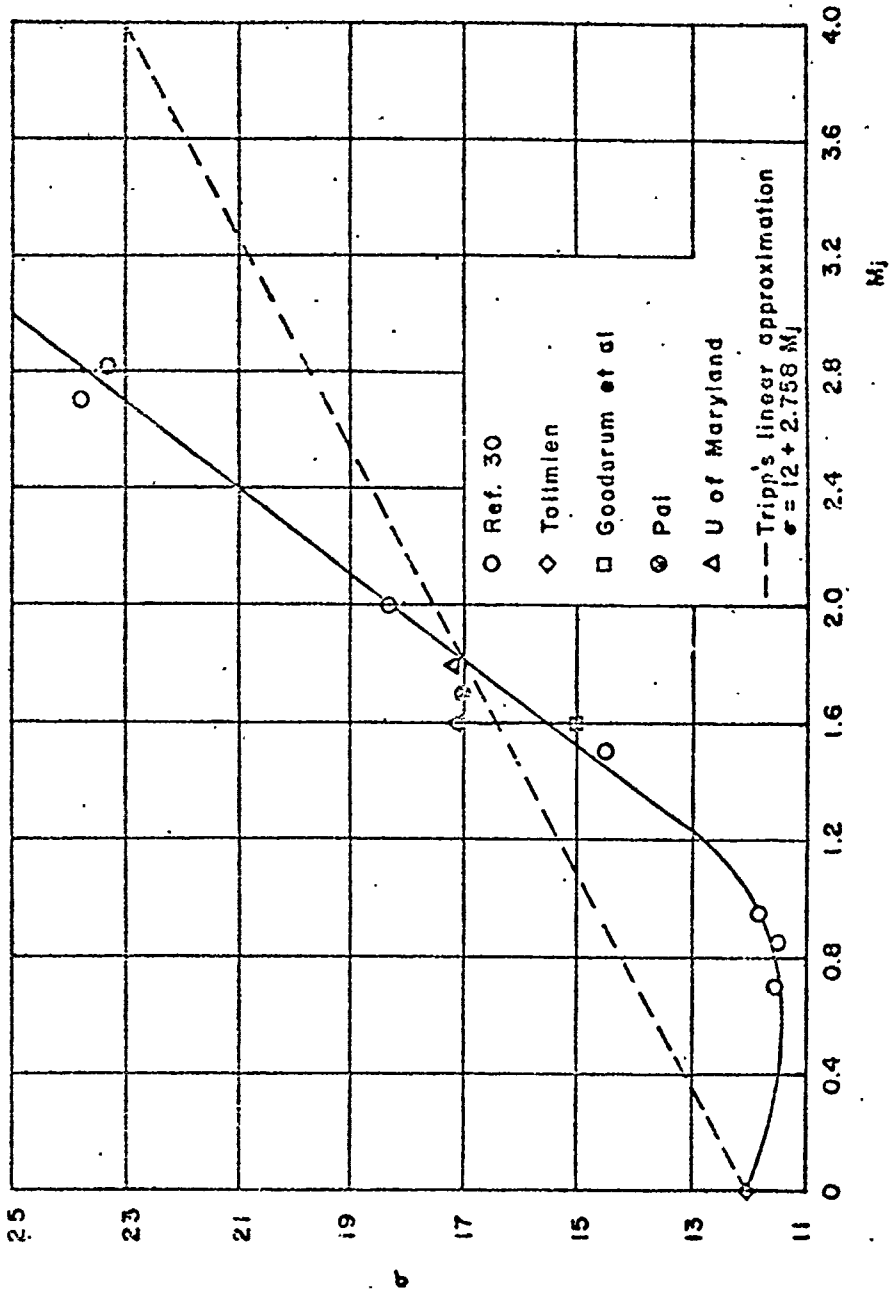

Fig.8 Effect of jet Mach number on the spreading rate parameter of a jet exhausting into a medium at rest

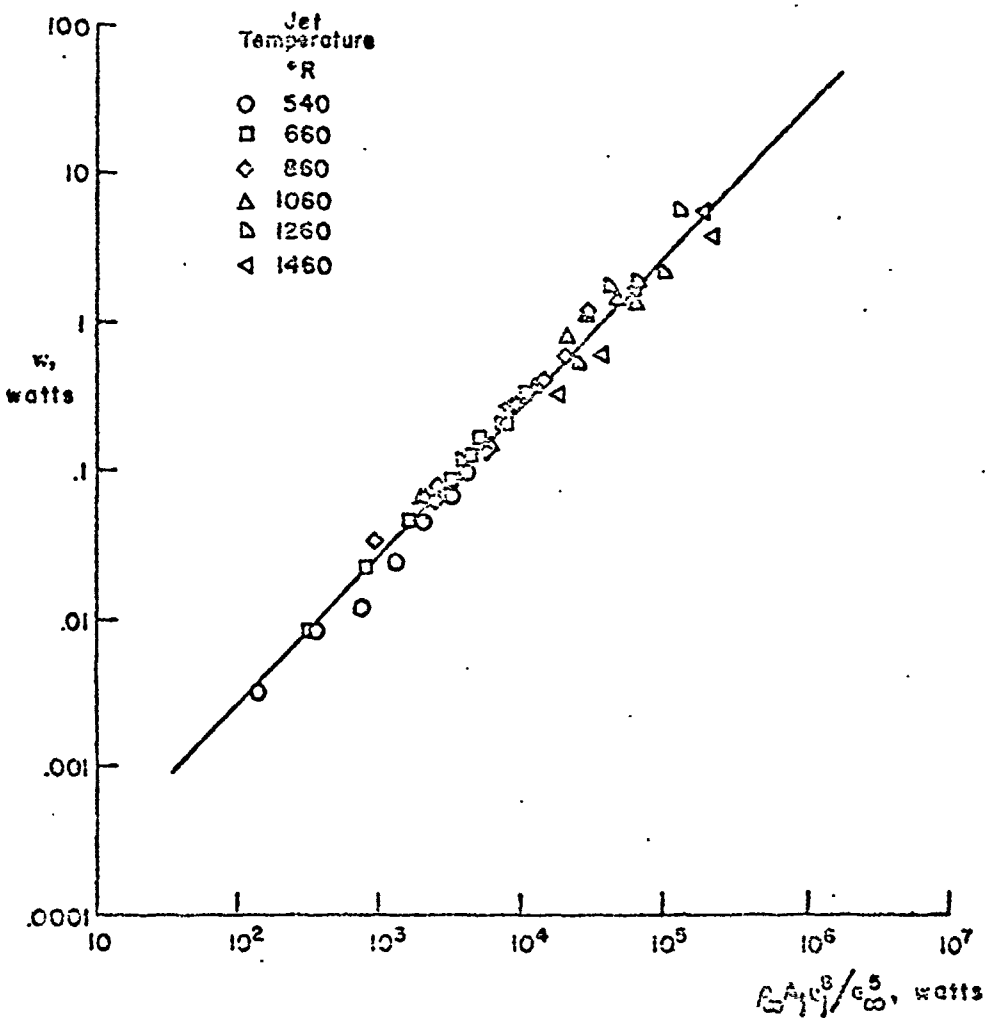

Fig.9 Effects on jet noise of a subsonic jet exhausting into a medium at rest

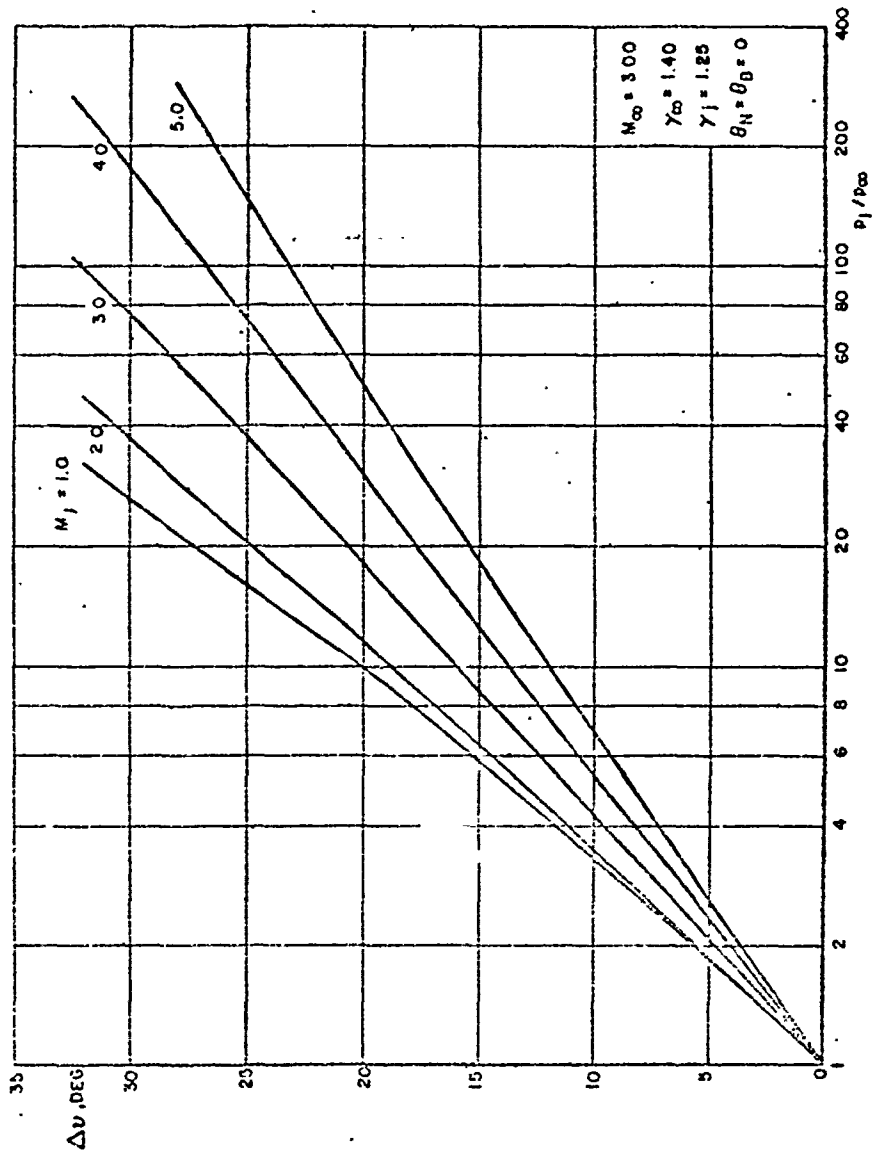

Fig.10 Effect of jet Mach number on the initial inclination angle of a jet exhausting into a moving stream

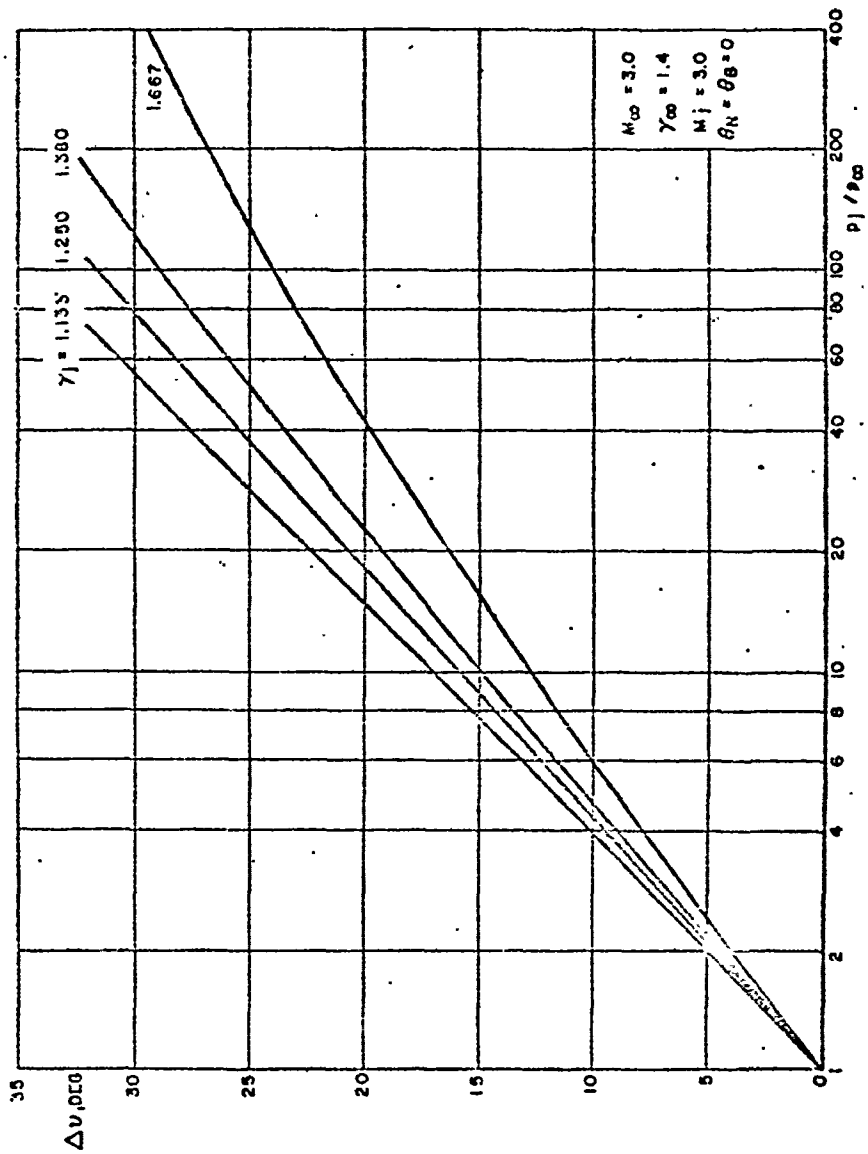

Fig.11 Effect of the ratio of specific heats of the jet on the initial angle of a jet exhausting into a moving stream.

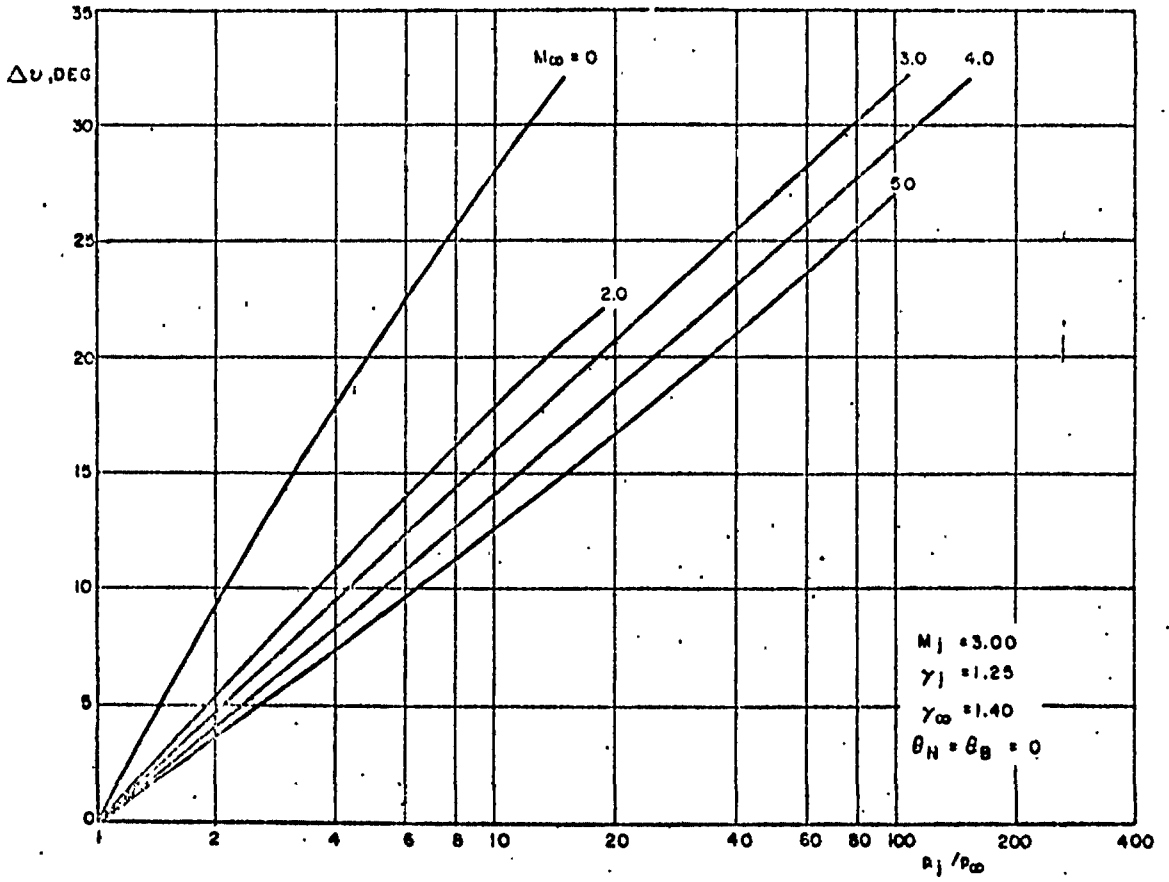

Fig.12 Effect of free stream Mach number of the initial inclination angle of a jet exhausting into a moving stream

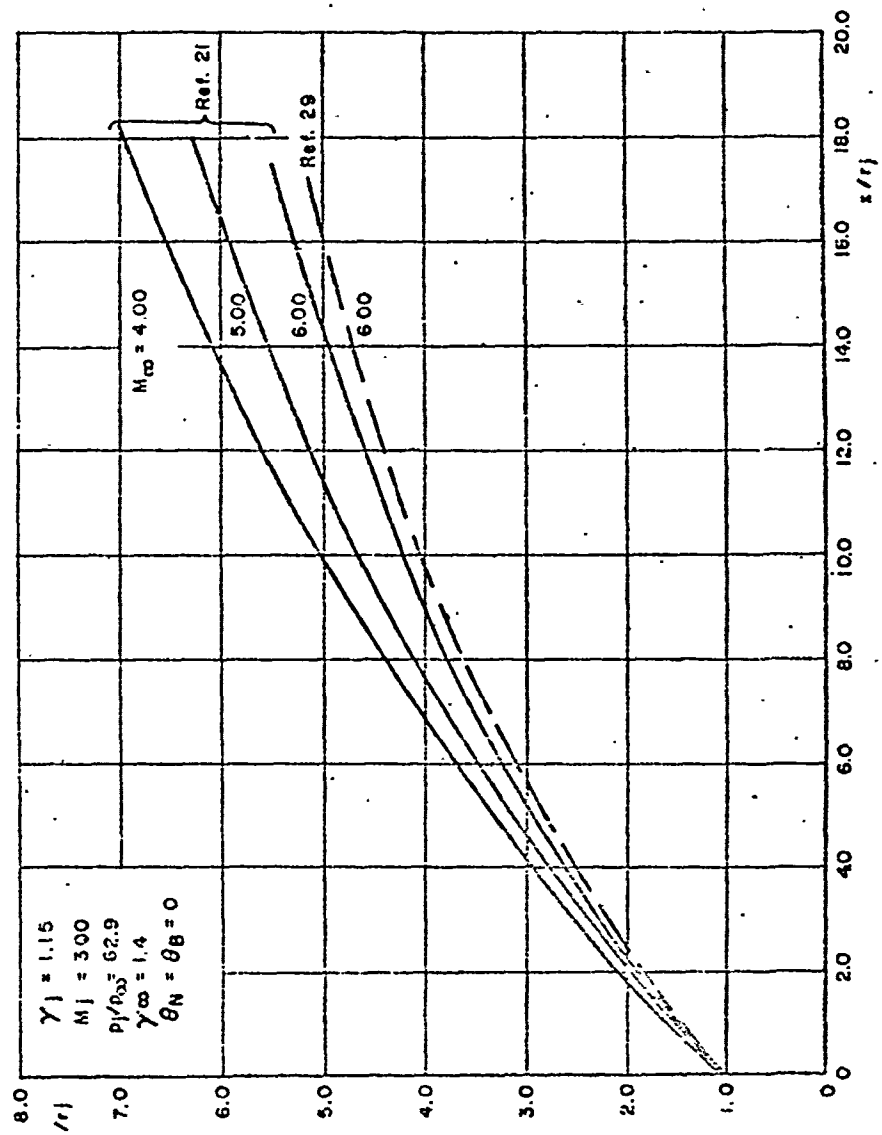

Fig.13 Effect of free stream Mach number on the boundary of a jet exhausting into a moving stream

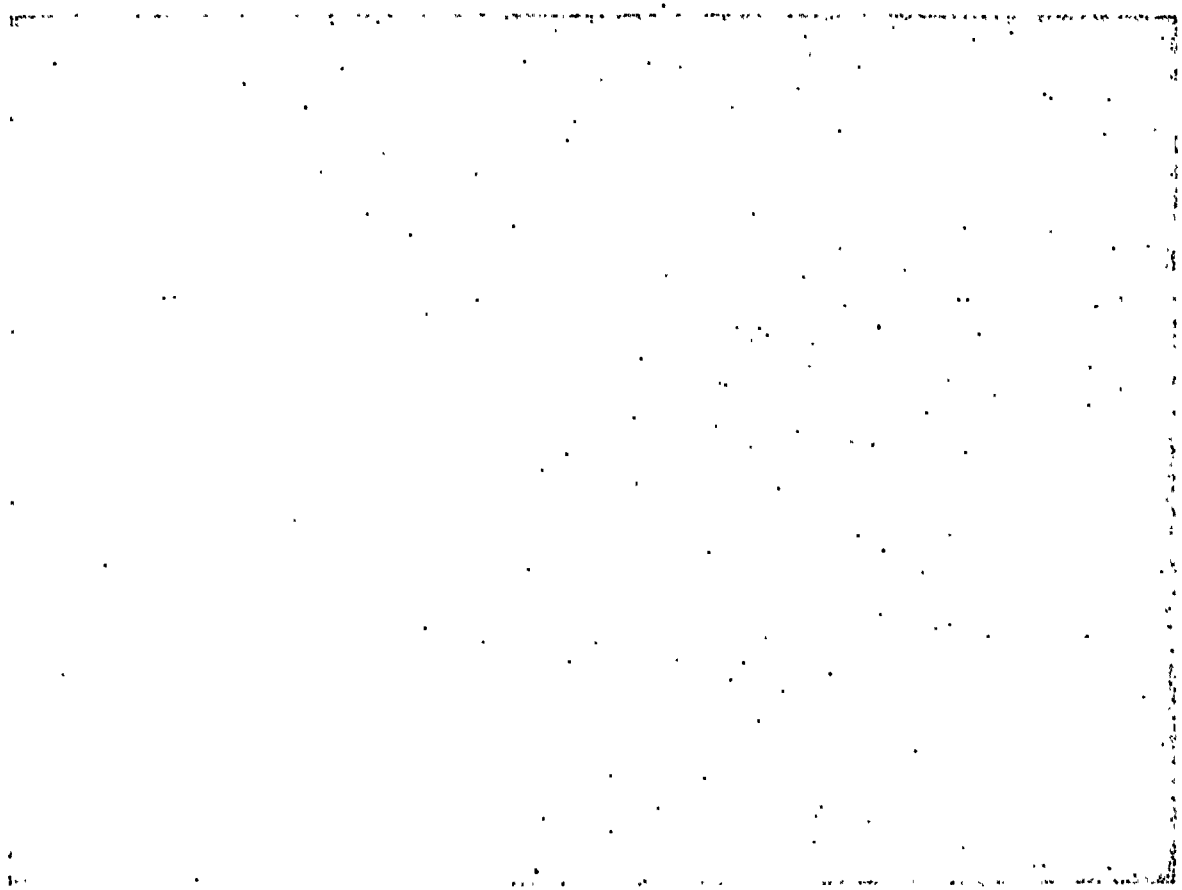

Fig.14 Typical Schlieren photograph of a jet exhausting into a moving stream

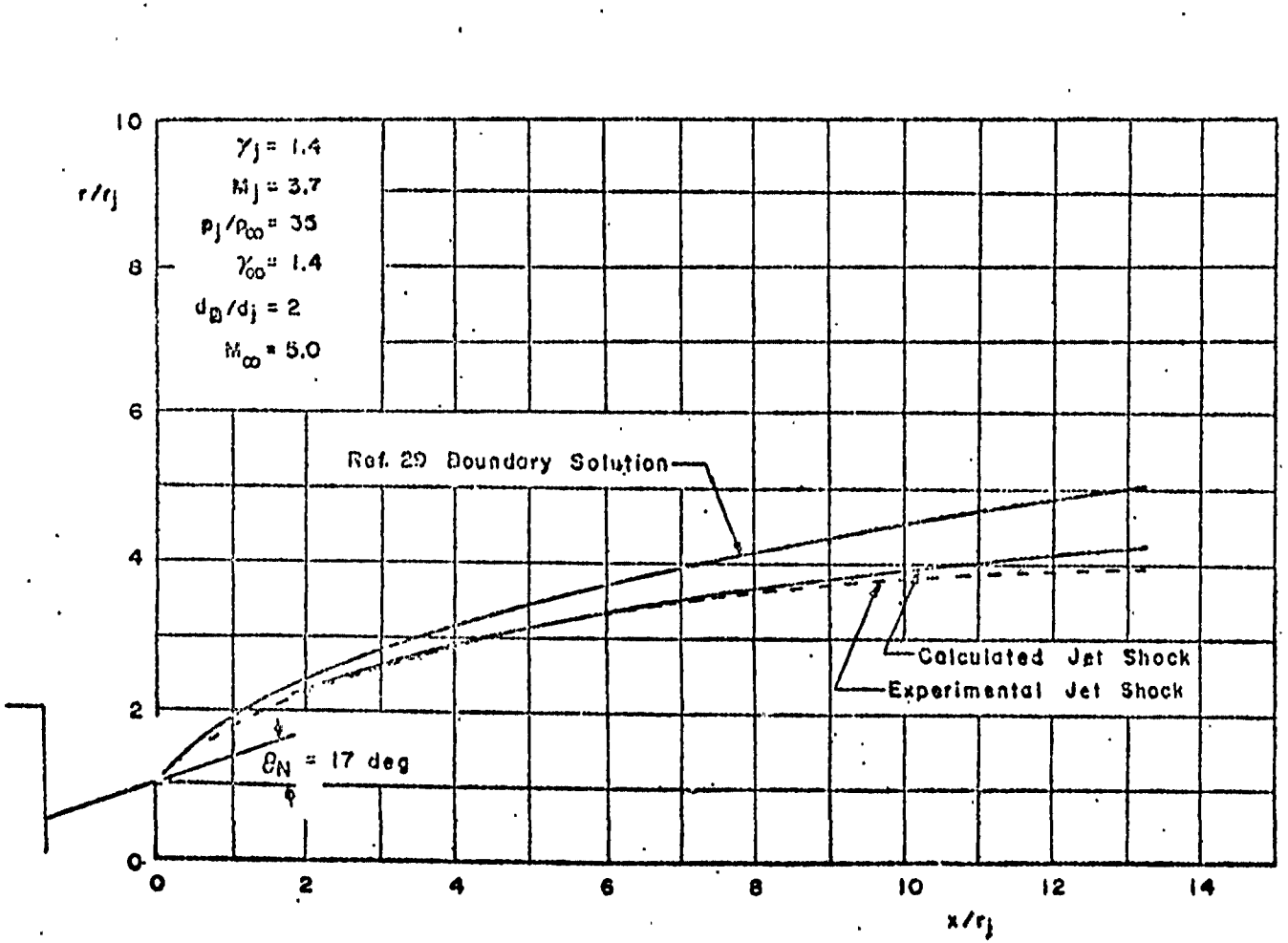

Fig. 15 Comparison of an experimental and calculated jet shock in a jet exhausting into a moving stream

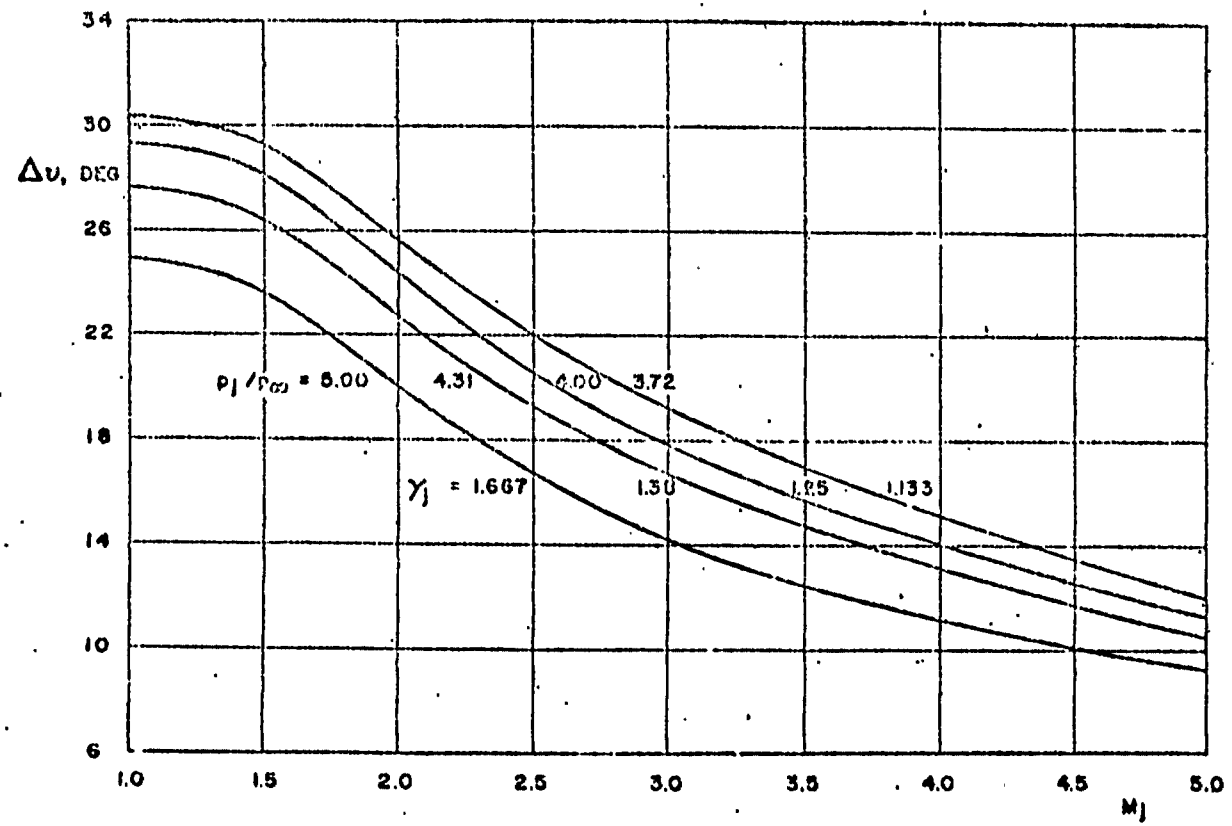

(a) $(p_j/p_\infty - 1)\dfrac{1}{\gamma_j} = 2.4$

Fig.16 Values of the initial inclination angle of a jet exhausting into a medium at rest using a constant jet Mach number similarity parameter

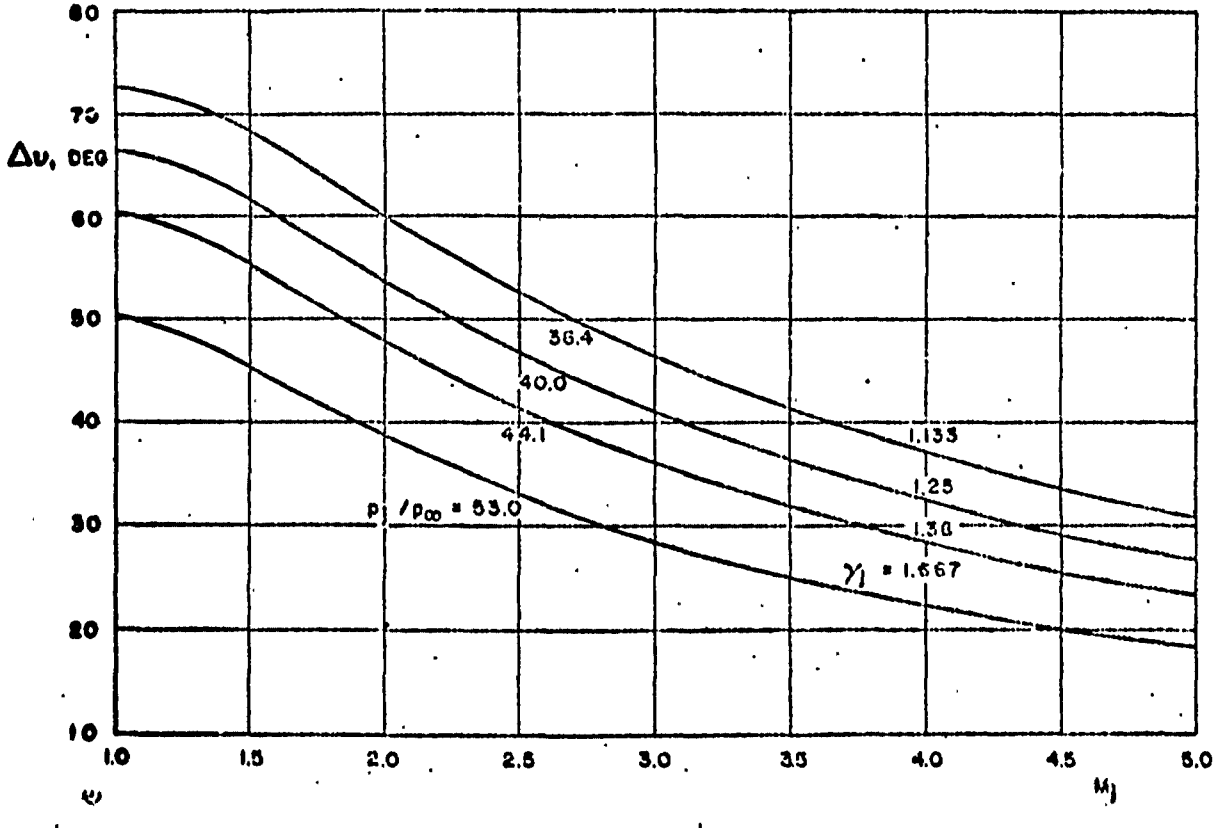

(b) $(p_j/p_\infty - 1)\frac{1}{\gamma_j} = 31.2$

Fig.16 Values of the initial inclination angle of a jet exhausting into a medium at rest using a constant jet Mach number similarity parameter

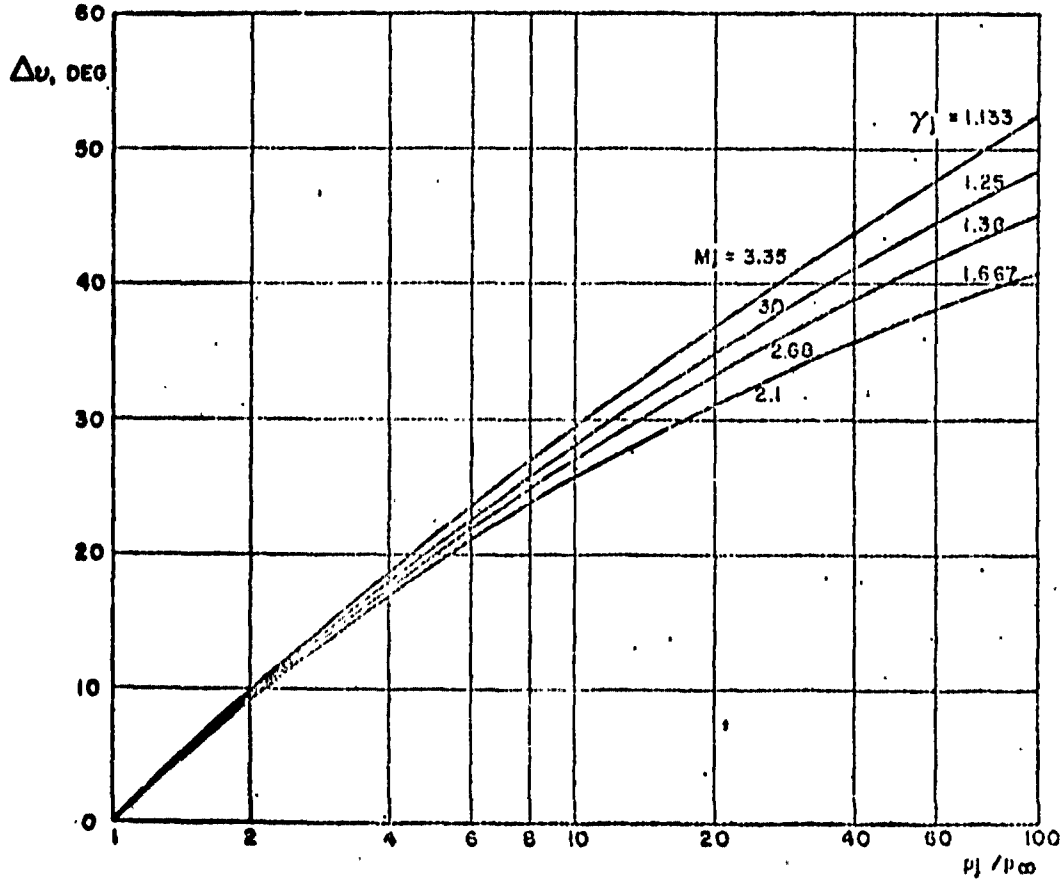

Fig.17 Values of the initial inclination angle of a jet exhausting into a medium at rest using a constant jet pressure ratio similarity parameter, $\gamma_j M_j^2/\beta_j = 3.98$

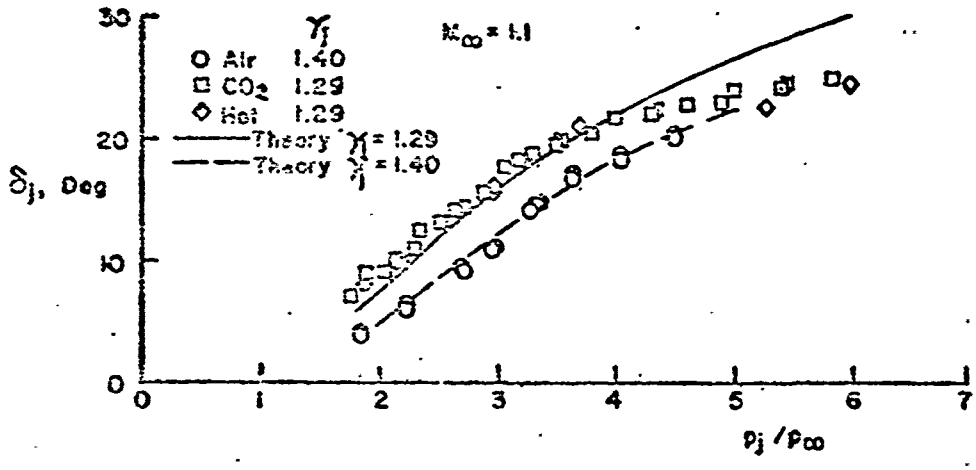

Fig.18 Initial inclination angle of a sonic jet exhausting into a moving stream

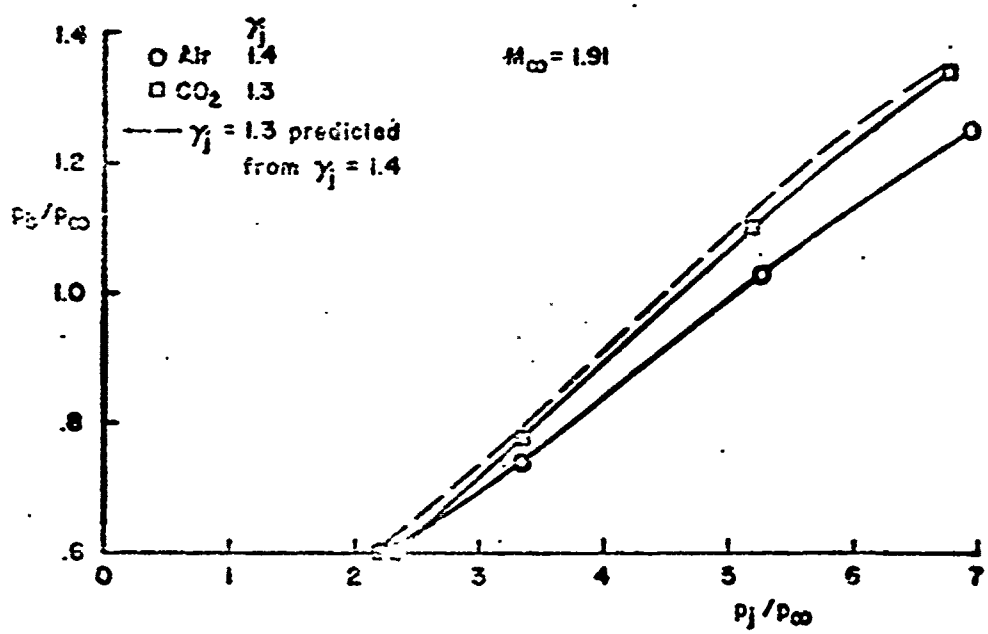

Fig.19 Effect of a sonic jet exhaust on base pressure

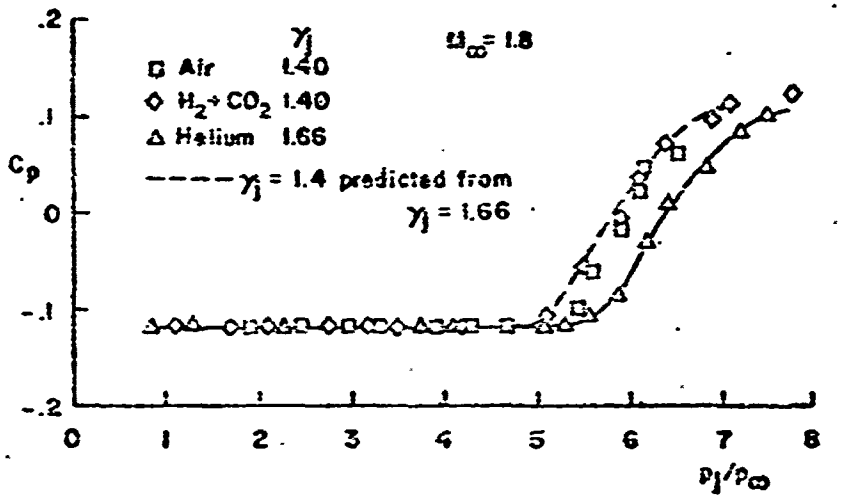

Fig.20 Effect of the exit shock from a sonic jet on the pressure coefficient at a point in a moving stream

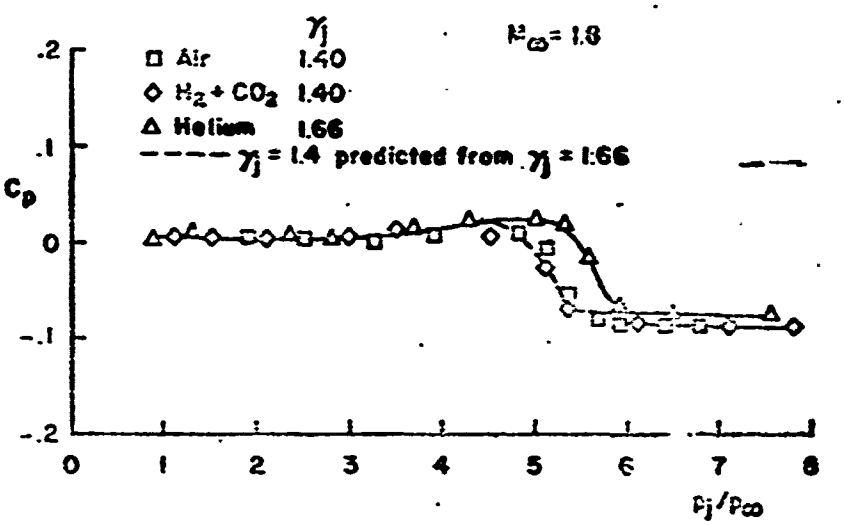

Fig.21 Effect of the transmitted shock from a sonic jet on the pressure coefficient at a point in a moving stream

DISTRIBUTION

Copies of AGARD publications may be obtained in the various countries at the addresses given below.

On peut se procurer des exemplaires des publications de l'AGARD aux adresses suivantes.

BELGIUM BELGIQUE	Centre National d'Etudes et de Recherches Aéronautiques 11, rue d'Egmont, Bruxelles
CANADA	Director of Scientific Information Service Defense Research Board Department of National Defense 'A' Building, Ottawa, Ontario
DENMARK DANEMARK	Military Research Board Defense Staff Kastellet, Copenhagen Ø
FRANCE	O.N.E.R A. (Direction) 25, Avenue de la Division Leclerc Châtillon-sous-Bagneux (Seine)
GERMANY ALLEMAGNE	Zentralstelle für Luftfahrt-dokumentation und -information München 27, Maria-Theresia Str. 21 Attn: Dr. H.J. Rautenberg
GREECE GRECE	Greek National Defense General Staff B. MEO Athens
ICELAND ISLANDE	Director of Aviation c/o Flugrad Reykjavik
ITALY ITALIE	Ufficio del Generale Ispettore del Genio Aeronautico Ministero Difesa Aeronautica Roma
LUXEMBURG LUXEMBOURG	Obtainable through Belgium
NETHERLANDS PAYS BAS	Netherlands Delegation to AGARD Schoolstraat 10 Delft

NORWAY NORVEGE	Mr. O. Blichner Norwegian Defence Research Establishment Kjeller per Lillestrøm
PORTUGAL	Col. J.A. de Almeida Viana (Delegado Nacional do 'AGARD') Direcção do Serviço de Material da F.A. Rua da Escola Politecnica, 42 Lisboa
TURKEY TURQUIE	Ministry of National Defence Ankara Attn. AGARD National Delegate
UNITED KINGDOM ROYAUME UNI	Ministry of Aviation T.I.L., Room 009A First Avenue House High Holborn London W.C.1
UNITED STATES ETATS UNIS	National Aeronautics and Space Administration (NASA) 1520 H Street, N.W. Washington 25, D.C.

Printed by Technical Editing and Reproduction Ltd
Harford House, 7-9 Charlotte St. London, W.1.

A[illegible] 79 [illegible] Atlantic Treaty Organization, Advisory Group f[illegible] autical Research and Development [illegible]ATION IN GROUND TEST FACILITIES [illegible]n [illegible], 1963 [illegible] incl. 69 refs. & 21 figs. [illegible]per presents a review of various techniques [illegible]lation of a jet exhaust in ground [illegible]ilities. A brief summary of the character-[illegible] of a jet exhausting into both quiescent and [illegible]edia is presented. The importance of [illegible]ating the initial inclination angle of the jet, δ_j, when conducting simulation studies is pointed out. Various scaling parameters are P.T.O.	533.6.072:533.697.4 3b1c 3b2e2	AGARDograph 79 North Atlantic Treaty Organization, Advisory Group for Aeronautical Research and Development JET SIMULATION IN GROUND TEST FACILITIES M. Pindzola November 1963 56 pp., incl. 69 refs. & 21 figs. This paper presents a review of various techniques employed in the simulation of a jet exhaust in ground test facilities. A brief summary of the characteristics of a jet exhausting into both quiescent and moving media is presented. The importance of duplicating the initial inclination angle of the jet, δ_j, when conducting simulation studies is pointed out. Various scaling parameters are P.T.O.	533.6.072:533.697.4 3b1c 3b2e2
[illegible] 79 [illegible] Atlantic Treaty Organization, Advisory Group [illegible] [illegible]utical Research and Development [illegible]ULATION IN GROUND TEST FACILITIES [illegible]n [illegible], 1963 [illegible] incl. 69 refs. & 21 figs. [illegible]per presents a review of various techniques [illegible] the simulation of a jet exhaust in ground [illegible]ilities. A brief summary of the character-[illegible] of a jet exhausting into both quiescent and moving media is presented. The importance of duplicating the initial inclination angle of the jet, δ_j, when conducting simulation studies is pointed out. Various scaling parameters are P.T.O.	533.6.072:533.697.4 3b1c 3b2e2	AGARDograph 79 North Atlantic Treaty Organization, Advisory Group for Aeronautical Research and Development JET SIMULATION IN GROUND TEST FACILITIES M. Pindzola November 1963 56 pp., incl. 69 refs. & 21 figs. This paper presents a review of various techniques employed in the simulation of a jet exhaust in ground test facilities. A brief summary of the characteristics of a jet exhausting into both quiescent and moving media is presented. The importance of duplicating the initial inclination angle of the jet, δ_j, when conducting simulation studies is pointed out. Various scaling parameters are P.T.O.	533.6.072:533.697.4 3b1c 3b2e2

enumerated. A requirement for the duplication of the jet pressure ratio, jet momentum, and the parameters $\gamma_j M_j^2 / \beta_j$ and $(RT)_j$ is indicated. Experimental data are also presented which verify the importance of these parameters in simulation studies. One method of selecting the geometry and test conditions for a simulation model in order to account for a difference in γ_j between model and full scale and still duplicate the important similarity parameters, is presented.

This is one of a series of publications by the AGARD-NATO Fluid Dynamics Panel.

enumerated. A requirement for the duplication of the jet pressure ratio, jet momentum, and the parameters $\gamma_j M_j^2 / \beta_j$ and $(RT)_j$ is indicated. Experimental data are also presented which verify the importance of these parameters in simulation studies. One method of selecting the geometry and test conditions for a simulation model in order to account for a difference in γ_j between model and full scale and still duplicate the important similarity parameters, is presented.

This is one of a series of publications by the AGARD-NATO Fluid Dynamics Panel.